UDC 576+546.922+547.496.3 doi: https://doi.org/10.15407/ubj96.03.075

IODIDE n,π-CHELATE COMPLEXES OF PLATINUM(II) BASED ON N-ALLYL SUBSTITUTED THIOUREAS AND THEIR EFFECT ON THE ACTIVITY OF HEPATOBILIARY SYSTEM ENZYMES IN COMPARISON WITH CHLORIDE ANALOGS

V. ORYSYK[1]✉, L. GARMANCHUK[2], S. ORYSYK[3], Yu. ZBOROVSKII[1], S. SHISHKINA[4], I. STUPAK[2], P. NOVIKOVA[3], D. OSTAPCHENKO[2], N. KHRANOVSKA[5], V. PEKHNYO[3], M. VOVK[1]

[1]Department of Functional Heterocyclic Systems Chemistry, Institute of Organic Chemistry, National Academy of Sciences of Ukraine, Kyiv;
[2]Department of Biomedicine of Taras Shevchencko National University, Educational and Scientific Centre "Institute of Biology and Medicine", Kyiv, Ukraine
[3]Department of Complex Compounds Chemistry, V.I. Vernadsky Institute of General and Inorganic Chemistry, National Academy of Sciences of Ukraine, Kyiv;
[4]Department of X-ray Diffraction Studies and Quantum Chemistry, SSI "Institute for Single Crystals", National Academy of Sciences of Ukraine, Kharkiv;
[5]National Cancer Institute, Kyiv, Ukraine;
✉e-mail: vis.viktorys@gmail.com

Received: 21 December 2023; **Revised:** 30 January 2024; **Accepted:** 31 May 2024

The search for new effective drugs in the treatment of neoplasm remains relevant even today, since the adaptation of transformed cells to the action of classical drugs contributes to the emergence of drug resistance. This applies to a number of classic chemotherapy drugs of the platinum series, in particular cisplatin. In this work, we describe the effect of novel analogs of cisplatin on HepG2 cells and on the key enzyme of antioxidant protection system gammaglutamyltranspeptidase, which plays an important role in the acquisition of drug resistance to anticancer drugs by tumor cells. New mononuclear iodide n,π-chelate complexes of Pt(II) with substituted thioureas N-allylmorpholine-4-carbothioamide or 3-allyl-1,1-diethylthiourea were obtained as analogs of cisplatin. All compounds were investigated by UV-Vis, IR, and $^{1}H/^{13}C$ NMR spectra. Complex I was described by single-crystal X-ray diffraction study. Also, the effect of these analogs on alanine aminotransferase, aspartate aminotransferase, lactate dehydrogenase, which are marker enzymes of liver cells, release of which into the blood indicates liver pathologies, was investigated. All studies were carried out in comparison with chloride n,π-chelate complexes of platinum obtained earlier (however, the effect of these chloride analogs of platinum on enzymes of the hepatobiliary system was investigated for the first time in this work). The results have shown that the studied compounds are better cytostatics/cytotoxics than cisplatin both according to IC_{50} and apoptosis level of HepG2 cells. It is established that, for the most part, effect of the studied complexes is reduced to a decrease in the degree of malignancy of cells of hepatocyte lines and the activity of LDH and GHT, as well as a decrease in consumed glucose.

K e y w o r d s: n,π-chelates; thioureas, NMR spectroscopy; crystal structure, gammaglutamyltranspeptidase, alanine aminotransferase, aspartate aminotransferase, lactate dehydrogenase.

Despite great efforts to improve the therapy of malignant diseases, in recent decades, the spectrum of available effective drugs is relatively limited (especially based on metal-containing), which is caused by their toxicity and the resistance of pathogenic cells to their action. So, there is a significant need for the development of new effective and less toxic anticancer agents [1-3]. Since the discovery of cisplatin by Barnett Rosenberg in 1960, metal complexes have provided a very versatile platform for the development of anticancer drugs. Most transition metal compounds have shown high antitumor activity, among which, in addition to platinum, less toxic metals such as ruthenium, pal-

ladium, gold, or copper have been used as possible candidates for obtaining more effective antitumor substrates [4, 5].

At the same time, numerous studies have shown that the choice of ligands is crucial, as they not only control the reactivity of the metal, but also determining the nature of interactions involved in the recognition of biological target sites such as DNA, enzymes and protein receptors [6]. Increasing attention has been given to the study of transition metals complexes with bi- and polydentate the nitrogen, oxygen and sulfur donor ligands that form stable substances of the chelate type. Such complex compounds have significant advantages over free ligands and inorganic salts, since coordination with chelating organic substances prevents hydrolysis under physiological conditions, reduces toxicity and increases solubility, which makes them promising objects for the design of new pharmaceuticals [7-9].

A recent trend in the development of new metal-based anticancer drugs is the use of biologically active ligands capable of inhibiting the growth of malignant tumors with different mechanisms of action [10, 11]. Promising ligands for the development of new potential drugs are thiourea derivatives, which, having high antitumor activity [12], are able to coordinate many metal ions as N,S donor agents [13-15]. In previous studies, we found that a number of π-coordination complexes of Pt(II) and Pd(II) with N-allylthiourea derivatives showed a high affinity to DNA with cytostatic and proapoptotic effects which was superior to that of cisplatin [16-19]. As a "carrier ligand" providing transport of these complexes to their target, we used the allylthiourea derivatives and the role of the leaving groups was performed by chlorine atoms. In the presented work, we obtained similar complexes in which, instead of chlorine atoms, the role of "leaving groups" is played by iodine atoms, which, as could be assumed, should be more easily amenable to nucleophilic substitution on nitrogen atoms of DNA nucleic bases. Earlier, we established that iodide platinum(II) π-complexes completely transformed the supercoiled form of DNA into a relaxed ring form even at a concentration of 12.5 μg/ml, which is much more effective than cisplatin [18]. Then we assumed that π-complexes of platinum with iodide anions in the coordination sphere interact with DNA the fastest.

The next step in the evaluation of the antitumor effect of such Pt(II) n,π-chelate complexes was the study of their influence on the activity of enzymes of the hepatobiliary system. Serum enzymes such as aspartate aminotransferase (AST), alanine aminotransferase (ALT), lactate dehydrogenase (LDH), and their isoenzymes can change their activity in liver pathology. ALT and AST are marker enzymes of liver cells. Normally, enzymes are active in the cell and their level in the blood is quite low. However, the release of the enzyme into the blood, which occurs as a result of the destruction of cells, indicates pathologies in the liver. After all, during the study of the effect of cisplatin and platinum-containing compounds on liver cells, the detection of the above-mentioned enzymes in the blood indicates the probable apoptosis of tumor cells and, therefore, the implementation of the intercalating function of platinum complexes.

As the results of our previous studies showed, complexes based on morpholine- and diethylamino-substituted thioureas were most effective for interacting with DNA [16, 17, 20]. Therefore, in this work, these ligands were used to obtain iodide n,π-chelate complexes. However, for greater clarity of their action, we compared the activity of new iodide pi-complexes, obtained for the first time in this work, with their chloride analogs, synthesized by us much earlier [16, 17, 20]. The aim of the work was to determine the effect of new iodide n,π-chelate complexes on the functional activity of HepG2 human hepatocarcinoma cells in comparison with their chloride analogs, the effect of which on the same cells had not been studied before, but was also presented for the first time in this work (previously, their effect on cells of the Hela and MCF7 lines was studied [16, 17, 20]).

In addition, the dependence of neoplastic cell viability on the presence of glucose in the environment has long been established. The rate of glucose absorption by a tumor is an order of magnitude (10-15 times) higher than that in healthy tissues, mainly due to the high expression of membrane glucose transporters and the excessively fast utilization of this monosaccharide. Ninety percent of the adenosine triphosphate (ATP) of the transformed cell is produced during the glycolysis process, which is mainly due to the anaerobic conditions in which tumors are located and the corresponding reprogramming of their metabolism. The Warburg effect describes the adaptation of tumor cells to conditions of deep hypoxia by turning on glycolysis. This contributes to the rapid growth of the neoplasm, however, due to the involvement of a high level of

glucose [21]. Therefore, the effect of synthesized compounds on the level of glucose absorption was also investigated in the present work.

At the same time, the resistance of pathogenic cells to the action of a number of chemotherapy drugs of the platinum series (such as cisplatin, oxaliplatin, carboplatin, nedaplatin, etc.) is known. In order to overcome this shortcoming, the selection of new agents aimed at various cellular targets is carried out in order to identify their multifunctional effect on the relevant signaling pathways with subsequent suppression of uncontrolled proliferation of pathogenic cells or induction of apoptotic and autophagic pathways of death of such cells.

Along with this, the normalization of the metabolic phenotype (suppression of anaerobic glycolysis, activation of oxidative phosphorylation, initiation of the mitochondrial link of apoptosis) of transformed cells of a heterogeneous tumor can affect proliferative indicators. It is known that the antioxidant defense system, in particular, the key enzyme of the glutathione system, gammaglutamyltranspeptidase (GGT), plays a key role in the acquisition of drug resistance to cisplatin by tumor cells. Therefore, in the presented work, a classical model was used for such experiments - transformed cells of the HepG2 line (human hepatocarcinoma) with a doubling time of 27 h.

Materials and Methods

Materials. Initial reagents $K_2[PtCl_4]$, KI, hydrochloric acid and solvents (ethanol and diethyl ether) used in this work were of synthetic grade and used as purchased in Merck without further purification.

N-Allylmorpholine-4-carbothioamide (HL^1) and 3-allyl-1,1-diethylthiourea (HL^2) were obtained as a white solid by the methods described in our previous works [16, 18, 19]. HL^1. M. p. 61–62°C, Yield: (89%). C, H, N, and S% [Calculated for $C_8H_{14}N_2OS$: C: 51.58, H: 7.58, N: 15.04, S: 17.21. Found: C: 51.47, H: 7.55, N: 15.11, S: 17.10]. IR bands (ν, cm^{-1}): 3224 ν(NH); 3076 $\nu_{as}(CH)_{allyl}$, 3042 $\nu_s(CH)_{allyl}$; 2963, 2930 $\nu_{as}(CH)_{CH2}$; 2910, 2851 $\nu_s(CH)_{CH2}$; 1531 δ(NH) + ν_{as}(NCN); 1430, 1405 νs(N-CS-N) + δ(CH); 1371-1309 $\delta_s(CH)_{CH3}$; 1268-1214 $\delta(CH)_{CH2}$; 1120 δ(N-C-N); 933 $\delta(CH)_{-C=CH}$; 885 ν(C=S). ^{1}H NMR chemical shifts (500 MHz, DMSO-d_6) δ, ppm: 7.874 br. m (1H, N^2H); 5.869 m (1H, $-C^7H=$); 5.117 d (1H, J 17.5 Hz, $=C^8H_{trans}$); 5.050 d (1H, J 10.5 Hz, $=C^8H_{cis}$); 4.172 m (2H, C^6H_2); 3.748 t (4H, J 5.0 Hz, $2C^{1,4}H_2$); 3.572 t (4H, J 4.5 Hz, $2C^{2,3}H_3$). ^{13}C NMR chemical shifts (125.75 MHz, DMSO-d_6) δ, ppm: 181.43 C^5; 135.36 C^7; 115.48 C^8; 52.23 C^6; 45.42 $C^{1,4}$; 28.98 $C^{2,3}$.

HL^2. M. p. 64–65°C, Yield: (93%). C, H, N, and S% [Calculated for $C_8H_{16}N_2S$: C: 55.77, H: 9.36, N: 16.26, S: 18.61. Found: C: 55.69, H: 9.38, N: 16.21; S: 18.53]. IR bands (ν, cm^{-1}): 3295 ν(NH); 3086 $\nu_{as}(CH)_{allyl}$, 3060 $\nu_s(CH)_{allyl}$; 2985, 2955 $\nu_{as}(CH)_{CH3}$; 2917, 2870 $\nu_s(CH)_{CH3}$; 1535, 1500 δ(NH) + ν_{as}(NCN); 1445, 1407; ν_s(N-CS-N) + δ(CH); 1374-1320 $\delta_s(CH)_{CH3}$; 1275-1208 $\delta(CH)_{CH2}$; 965 $\delta(CH)_{-C=CH}$; 845 ν(C=S). ^{1}H NMR chemical shifts (500 MHz, DMSO-d_6) δ, ppm: 7.446 w.m (1H, N^2H); 5.879 m (1H, $-C^7H=$); 5.083 d (1H, J 17.0 Hz, $=C^8H_{trans}$); 5.036 d (1H, J 10.5 Hz, $=C^8H_{cis}$); 4.172 br.m (2H, C^6H_2); 3.621 m (4H, $2C^{1,4}H_2$); 1.098 t (6H, J 7 Hz, $2C^{2,3}H_3$). ^{13}C NMR chemical shifts (125.75 MHz, DMSO-d_6) δ, ppm: 180.05 C^5; 136.46 C^7; 115.26 C^8; 47.92 C^6; 44.68 $C^{1,4}$; 13.16 $C^{2,3}$.

All the complexes were synthesized according to the following general methodic: A portion of $K_2[PtCl_4]$ (103.7 mg, 0.25 mmol) was dissolved in 1 ml of distilled water and 0.5 ml of 2N HCl was added. The resulting solution was made up to a volume of 5 ml with distilled water and then an excess of dry potassium iodide salt (332 mg, 1 mmol) was added with constant stirring and heating (50-60°C) for 15 min. 10 ml of a warm ethanolic solution of thiourea HL^1 or HL^2 (0.25 mmol) was added dropwise to the resulting solution with constant stirring. The mixture was stirred without heating for 25 min and left for crystallization. The formed dark red (complex **I**) or light brown (complex **II**) crystals were filtered and washed with ethanol and diethyl ether. Yields were 65-70%. Crystals of complex **I**, suitable for single-crystal X-ray diffraction study, were formed on day 5. The decomposition temperature of both complexes is > 320°C. The purity of the products was assessed through elemental percentages of C, H, N, and S.

$[Pt(HL^1)I_2]\times H_2O$ (I). Yield: (70 %). C, H, N, and S% [Calculated for $C_8H_{16}I_2N_2O_2PtS$: C: 14.71, H: 2.47, I: 38.86, N: 4.29, S: 4.91. Found: C: 14.93, H: 2.50, I: 39.03, N: 4.35, S: 5.00]. IR bands (ν, cm^{-1}): 3450-3575 w. $\nu(OH)_{H2O}$; 3275 ν(NH); 3125 $\nu_{as}(CH)_{allyl}$, 3075 $\nu_s(CH)_{allyl}$; 2963, 2923 $\nu_{as}(CH)_{CH2}$; 2910, 2858 $\nu_s(CH)_{CH2}$; 1567 δ(NH) + ν_{as}(NCN); 1430, 1396; ν_s(N-CS-N) + δ(CH); 1334-1305 $\delta_s(CH)_{CH2}$; 1276-1210 $\delta(CH)_{CH2}$; 1100 δ(N-C-N); 978 $\delta(CH)_{C=CH}$; 870 ν(C=S). ^{1}H NMR chemical shifts (400 MHz, DMSO-d_6) δ, ppm: 9.240 br. m (1H, N^2H); 5.456 m (1H, $-C^7H=$); 4.073 d (1H, J 12.4 Hz, $=C^8H_{trans}$); 4.607 d

(1H, J 7.6 Hz, =C^8H_{cis}); 3.774 m (2H, C^6H_2); 3.677 m (4H, $2C^{1,4}H_2$); 3.391 m (4H, $2C^{2,3}H_3$). ^{13}C NMR chemical shifts (125.75 MHz, DMSO-d_6) δ, ppm: 166.28 C^5; 80.26 C^7; 64.66 C^8; 51.21 C^6; 43.53 $C^{1,4}$; 28.68 $C^{2,3}$.

[Pt(HL$_2$)I$_2$] (II). Yield: (65 %). C, H, N, and S% [Calculated for C8H16I2N2PtS: C: 15.47, H: 2.60, I: 40.86, N: 4.51, S: 5.16. Found: C: 15.35, H: 2.68, I: 40.70, N: 4.38, S: 5.05]. IR bands (ν, cm^{-1}): 3320 ν(NH); 3130 $\nu_{as}(CH)_{allyl}$, 3073 $\nu_s(CH)_{allyl}$; 2975, 2930 $\nu_{as}(CH)_{CH3}$; 2865 $\nu_s(CH)_{CH3}$; 1490 δ(NH) + ν_{as}(NCN); 1453, 1425; ν_s(N-CS-N) + δ(CH); 1393-1347 $\delta_s(CH)_{CH3}$; 1291-1205 $\delta(CH)_{CH2}$; 1145 δ(N-C-N); 990 $\delta(CH)_{-C=CH}$; 800 ν(C=S). ^{1}H NMR chemical shifts (400 MHz, DMSO-d6) δ, ppm: 8.820 w.m (1H, N^2H); 5.452 m (1H, –C^7H=); 4.071 d (1H, J 17.6 Hz, =C^8H_{trans}); 4.586 d (1H, J 7.6 Hz, =C^8H_{cis}); 3.885 d (1H, J 13.2 Hz) and 3.700 d (1H, J 18.0 Hz) C^6H_2; 3.542 m (4H, $2C^{1,4}H_2$); 1.161 t (6H, J = 7.2 Hz, $2C^{2,3}H_3$). ^{13}C NMR chemical shifts (125.75 MHz, DMSO-d_6) δ, ppm: 167.92 C^5; 81.93 C^7; 61.36 C^8; 46.70 C^6; 40.56 $C^{1,4}$; 13.16 $C^{2,3}$.

Methods. Elemental analyses for carbon, hydrogen, nitrogen, and sulfur were performed by Carlo Erba Elemental Analyzer (Model 1106). The chlorine was measured by the Schoniger method. ^{1}H/^{13}C NMR spectra were measured on a Bruker Avance DRX-400 (or DRX-500) spectrometer (400.00, 500.00/125.75 MHz) in DMSO-d_6 solution using tetramethylsilane (TMS) as internal standard. Attenuated total internal reflection Fourier transform infrared (ATR-FT-IR) spectra were recorded on a Thermo Nicolet Nexus 4700 FT-IR spectrometer in a range of 4000-500 cm^{-1}.

UV-Vis spectra of ethanol-DMF (5:1) solutions of ligands (HL^1, HL^2) and complexes **I**, **II** were measured on a Spectrometer Shimadzu UV-3600 in a range of 200–800 nm in quartz cuvettes with l = 0.1 and 1 cm. The studies of complex formation in water-ethanol solutions were performed using spectrophotometric titration and the method of isomolar series [22]. The starting solutions (1×10^{-3} M) for titration were prepared by dissolving the exact weighed sample of K_2PtCl_4 in 2 ml of 2M HCl, and the compounds HL^1 or HL^2 in EtOH and brought to a volume of 25 ml with ethanol. A solution of potassium iodide (4×10^{-3} M) was prepared by dissolving an exact amount of salt in distilled water. Herewith the concentration of metal salts (CM) was constant (13.3×10^{-5} M for K_2PtCl_4 and 26.6×10^{-5} M for KI), while the concentration of carbothioamides HL^1/HL^2 was changed from 3.3×10^{-5} to 40×10^{-5} M. Working solutions were heated at 60-70°C for 10 min. After cooling to room temperature, their optical density was measured in quartz cuvettes with a thickness of 0.1 cm.

S*ingle-crystal X-ray diffraction.* For the structures of complex (**I**), X-ray intensity data were collected at 193 K, on the Bruker APEX II diffractometer (graphite monochromated MoKα radiation, CCD detector, φ- and ω-scanning, $2\Theta_{max}$ = 60°). The structure was solved by the direct method using SHELXTL package [23]. The absorption correction was done using 'multi-scan' method (T_{min} = 0.214, T_{max} = 0.747). The restrictions have been applied for the refinement of bond lengths in the disordered fragment (Pt–S distance is 2.27 Å). Positions of the hydrogen atoms were calculated geometrically and refined using "riding" model with U_{iso} = nU_{eq} (n = 1.5 for water molecule and n = 1.2 for other hydrogen atoms) of the carrier atom. Full-matrix least-squares refinement against F^2 in anisotropic approximation for non-hydrogen atoms using 4378 reflections was converged to wR_2 = 0.252 (R_1 = 0.093 for 3908 reflections with F>4σ(F), S = 1.311).

Crystal data for complex (I). The red crystals of the complex (I) are monoclinic, space group $P2_1/c$, $C_8H_{14}I_2N_2OPtS,H_2O$, M = 653.18, a = 8.3181(2), b = 8.2275(2), c = 21.9200(6) Å, β = 92.051(2)°, V = 1499.18(7) Å^3, Z = 4, d_{calc} = 2.894 g/cm^3, μ(MoK_α) = 13.607 mm^{-1}, F(000) = 1176, collected reflexes 26929 (4378 independent, R_{int} = 0.064).

The final atomic coordinates, and crystallographic data for complex (**I**) have been deposited with the Cambridge Crystallographic Data Centre, 12 Union Road, CB2 1EZ, UK (fax: +44-1223-336033; e-mail: deposit@ccdc.cam.ac.uk) and are available on request quoting the deposition numbers CCDC 2281169).

In vitro proteins activity. Cell line HepG2 (ECACC catalog no. 85011430) - human hepatocarcinoma cells are suitable for modeling *in vitro* system for studying polarized human hepatocytes, studying intracellular exchange and dynamics of bile tubule, sinusoidal membrane proteins and lipids in human hepatocytes *in vitro* [24-26].

Human cervix cancer line Hela cells (ECACC catalog no.93021013) were used to determine cytotoxic/cytostatic effects of target complexes.

In order to obtain the most extensive information about the effect of synthesized n,π-chelate complexes of Pt(II) based on N-allylthioureas on the metabolic indicators of HepG2 cells, the activity of

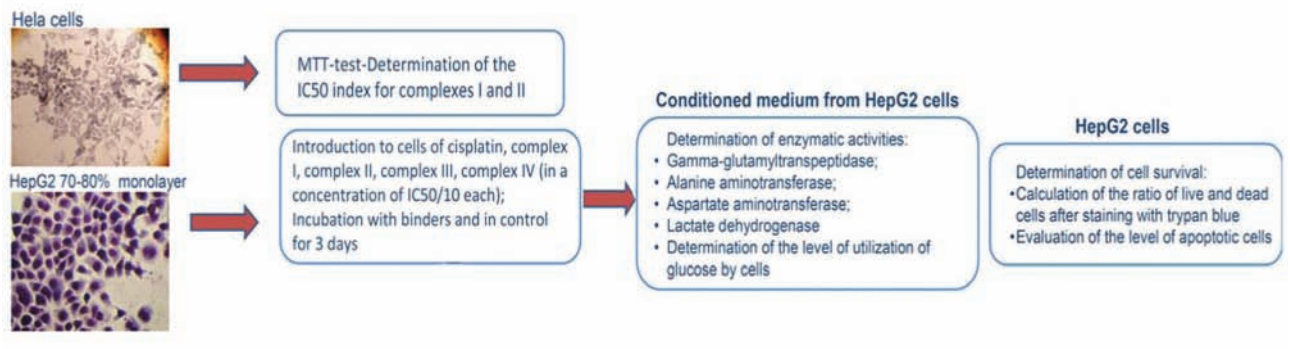

Fig. 1. Scheme of biological testing

a number of enzymes (such as alanine aminotransferase (ALT), aspartate aminotransferase (AST), lactate dehydrogenase (LDH), gamma-glutamyltranspeptidase (GGT)) and the level of glucose absorption were investigated according to scheme (Fig. 1).

MTT test. Determination of the cytotoxic/cytostatic effect on Hela cells under the influence of the components was carried out using the MTT test [27]. For this purpose, cells were planted in RPMI 1640 medium (Sigma, USA) containing 10% fetal bovine serum (FBS) and 10 ng/ml antibiotic/antimycotic mixture at a concentration of 1×10^5 cells/ml in a volume of 100 µl. The investigated complexes were added in successively decreasing concentrations to the wells of a 96-well tablet with cells and incubated for 24 h. In the control wells there was a medium without the tested substances (negative control). Four hours before the end of the incubation period, MTT reagent (colorless tetrazolium salt (Sigma Chemical Co., USA)) was added in 20 µl to a final concentration of 0.6 mM and incubated in a CO_2 incubator under standard conditions for the recovery of soluble MTT reagent by cells to insoluble formazan crystals. The plate was gently shaken for 5–10 min to dissolve the formazan crystals and the optical density of each well was determined at 540 nm (using a BioTek reader, USA) by subtracting the measured background absorbance at 620 nm. Results were reported as a percentage of the values obtained for the control sample [28]. Calculation of the concentration ratio of live and dead cells was carried out by the usual counting in the Horyaev chamber after staining the dead cells with trypan blue.

Obtaining conditioned culture medium of HepG2 cells and determination of key metabolic enzymes' activity, and glucose level. The culture mediums of HepG2 were investigated under the influence of the studied substances in concentrations $IC_{50}/10$ ($[Pt(HL^1)I_2]$ (**I**) – 3×10^{-6} M and $[Pt(HL^2)I_2]$ (**II**) – 5×10^{-7} M, respectively. Also for comparison, we used previously synthesized chloride π-complexes with concentrations $IC_{50}/10$ ($[Pt(HL^1)Cl_2]$ (**III**) – 1×10^{-6} M and $[Pt(HL^2)Cl_2]$ (**IV**) – 2.5×10^{-6} M, respectively [16]. Cisplatin at a concentration of 5.7×10^{-6} M was used as a comparison drug [16]. To do this, cells were planted in 6-well plates at a concentration of 2×10^5 cells/ml in a volume of 2 ml, incubated until reaching almost 100% confluency in a standard RPMI 1640 medium (Sigma, USA) containing 10% FBS, after which the medium was replaced with serum-free, the studied complexes were added, incubated for 2 days and determined the content of enzymes and metabolites. The metabolites secreted into the culture medium (cell secretome) were studied for fermentative activity, glucose level, and the level of apoptosis in cells. For this, cells were cultured for two days with complexes, culture medium was selected, and enzyme activity was analyzed.

The activity of key metabolic enzymes and the level of glucose in the medium of HepG2 cells under the action of new synthesized complexes were determined according to the recommendations of the manufacturer of the kits (Filisit, Ukraine).

Determination of the level of glucose in the incubation medium of the cells culture was performed at the end of day 2 of cultivation with both complexes. Initial cell concentration was 1×10^5 cells/ml in the sample volume of 200 µl. Measurement of glucose level (mmol) was carried out using a standard set based on the glucose-oxidase reaction, which we modified for culture medium of cells [29]. The intensity of glucose absorption was assessed by the decrease in its amount in the medium.

Determination of lactate dehydrogenase (LDH) and gamma-glutamyltranspeptidase (GGT) activi-

ty. Determination of LDH activity was assessed on day 2 by the spectrophotometric method according to the rate of NADH oxidation during the reduction of pyruvic acid (pyruvate + NADH + H^+ ↔ L–lactate + NAD^+) [30]. The samples were incubated with pyruvate and Nicotinamide adenine dinucleotide (NADH), and then the decrease in NADH absorption at 340 nm was measured. The reduction in the extinction (ΔE) by 1 μmol min^{-1} (μ = micro, $\times 10^{-6}$). The results were presented in μM/(min·ml).

The principle of the method determination of GGT activity is that under the influence of GGT, the glutamine residue from γ-*L*(+)-glutamine *p*-4-nitroanilide transfers to the dipeptide acceptor glycylglycine [31]. At the same time, a chromogen – *p*-nitroaniline - is released. The optical density of the reaction solution was measured after stopping the enzymatic reaction with a solution of acetic acid at a wavelength of 405 nm. The calculation is carried out according to the formula: $C=E_d/E_{ca}l \cdot 3.0$ [μkat/l], where C is GGT activity, μkat/l; 3 – conversion factor, μkat/l; E_d is the optical density of the test sample, units wholesale densities; E_{cal} is the optical density of the calibration sample, units wholesale density).

Determination of alanine aminotransferase (ALT) and aspartate aminotransferase (AST) activity. Determination of the activity of the main enzymes of the hepatobiliary system was carried out in the incubation medium according to classical methods [32, 33]. Alanine aminotransferase catalyzes the transfer of an amino group from alanine to 2-oxyglutarate with the formation of glutamate and pyruvate. The pyruvate formed in the presence of lactate dehydrogenase (LDH) is converted into lactate, with parallel oxidation of NADH.

α–oxyglutarate + L-alanine → L-glutamate + pyruvate:

Pyruvate + NADH + H^+ → lactate + NAD^+.

The following reagents were used for this reaction: L-alanine 400 mmol/l; LDH- 2000 U/l; NADH 0.25 mmol/l; α – oxyglutarate 12 mmol/l. 500 μl of the reagent was added to the test tube and 50 μl of the sample was added. The sample was mixed with the reagent immediately before the analysis. The rate of decrease in absorbance at 340 nm is directly proportional to the activity of ALT.

In the experiments, the kinetic method of determining the activity of aspartate aminotransferase was used [34] which corresponds to the recommendations of experts of the International Union of Clinical Chemistry (IFCC), according to which 2-ketoglutarate + L-aspartate ↔ L-glutamate + oxaloacetate oxaloacetate + NADH + H^+ ↔ L-malate + NAD^+. For this, the following reagents were used: *Tris*-buffer (pH 7.5) 80 mmol/l; L-aspartate 240 mmol/l; LDH 600 U/ml; MDG 600 U/ml; NADH 0.18 mmol/l; reagent 2 (substrate); 2-ketoglutarate 12 mmol/l; 500 μl of reagent 1 and 100 μl of reagent 2 were added to the test tube and 50 μl of conditioned medium for cell incubation was added. Next, the reagent was added to the resulting mixture immediately before the analysis, and AST activity was measured at λ 340 nm.

The level of HepG2 cell apoptosis after incubation with investigated complexes was determined by the generally accepted flow cytometric method, with use of Propidium Iodide (PI) [35]. PI binds to DNA by intercalating between the bases, with a stoichiometry of one dye per 4-5 base pairs of DNA.

Staining cells with the fluorochrome dye PI included the following stages: cells in the amount of 10^5 cells per sample after a single washing in 5 ml of Phosphate-buffered saline (PBS) at 400 g for 10 min was resuspended in 200 μl PBS and 300 μl Triton X-100 solution (0.1% sodium citrate, 0.1% Triton X-100). PI was added at 25 μl (0.5 μg/μl) to each sample. All reagents were provided by the company Sigma, USA. After careful shaking, the cells were incubated at 37°C for 30 min of darkness. Samples were washed with 20 ml PBS at 400 g for 10 min with supernatant removal. The pellet was fixed by adding 400 μl of 0.4% formalin solution in PBS. Sample measurements were performed no later than 3 days on flow cytometer FACS Calibur (Becton Dickinson, USA) with 488 nm argon laser and 582/42 nm narrowband filter in order to measure the fluorescence of PI. Flow cytometry data were analyzed using software Mod Fit LT 3.0 (Becton Dickinson, USA). The method of determining the level of apoptosis is based on the known fact that apoptotic cell death is preceded by extensive DNA fragmentation into oligonucleosomal subunits. Apoptotic cells presented as a broad hypodiploid DNA peak, which was easily discriminable from the narrow peak with normal (diploid) DNA content in the red fluorescence channels.

Results and Discussion

Chemistry. n,π-Chelate complexes $[Pt(HL^{1,2})I_2]$ have been obtained for the first time according to Scheme 1 by the reactions of $K_2[PtCl_4]$ with N-allylmorpholine-4-carbothioamide (HL^1) or 3-allyl-1,1-

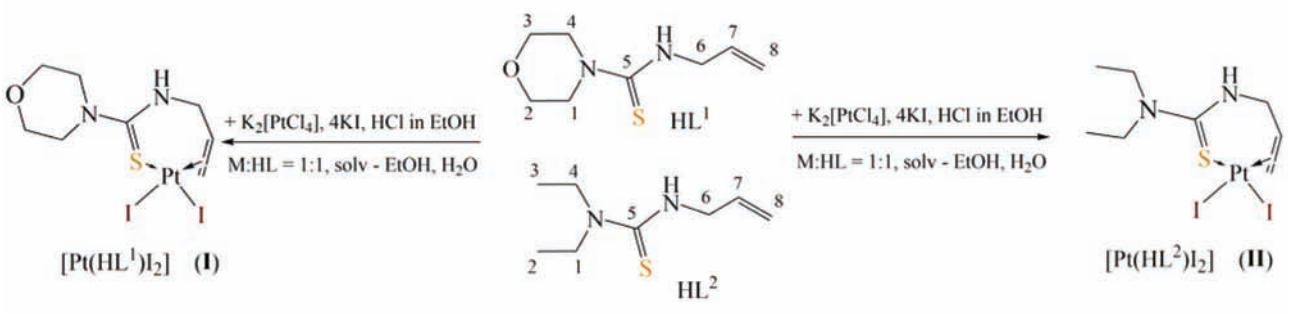

*Scheme 1. Synthesis of platinum(II) complexes **I**, **II***

diethylthiourea (HL^2) in the presence of HCl (to avoid hydrolysis of platinum and stabilize the surrounding metal with chloride ions [36, 37]) and a significant excess of KI to ensure anion exchange.

As in our previous works [16-19] a feature of the structure of both complexes is coordination of thioureas HL^1 and HL^2 in a bidentate-chelate manner by the atoms of the S,C-allylthiourea group, and the *cis*-position of iodide anions in the coordination sphere of the metal (Scheme 1).

Single-crystal X-ray structural analysis. According to the single-crystal X-ray diffraction study of complex **I** (Fig. 2, *a*), the Pt atom as well as one from the iodide atoms are disordered over two positions with a ratio of 92 : 8%.

In both positions, the Pt atom has a distorted square-planar coordination polyhedron formed by the sulfur atom of the thiourea group, π-system of the allyl group and two iodide anions. Complex **I** exists as monohydrate in the crystal phase. The value of the hydrogen bond O^{1w}…HN^2 is 1.98 Å. Similarly to the previously synthesized chloride analog [16], the C^8–C^7 double bond of the allyl fragment is placed perpendicular to the plane of the coordination polyhedron of the central atom (the angles I^{1A}-Pt^{1A}-C^8 and I^{1A}-Pt^{1A}-C^7 are 87.6(6)º and 89.6(5)º) which ensures the maximum overlap of the electronic π-orbitals of the ligand with the *d*-orbitals of the metal. The morpholine ring has an equatorial-chair conformation [37]. The carbothioamide HL^1 is in the thione tautomeric form, as indicated by the value of C^5-S^1 bond (1.74(2) Å). Its coordination to a metal ion led to elongation of bonds C^5-S^1 and C^7-C^8 (compared to the free ligand [16]) by 0.05 and 0.12 Å. Careful analysis of the bond distances and angles revealed the similarity in the C^8–Pt^{1A}–I^2 (164.1(6)°) and C^7–Pt^{1A}–I^2 (158.4(5)°) angles, which, in addition to the identical Pt^{1A}–C^8 and Pt^{1A}–C^7 (2.18(2) Å) bond distances in complex, allows the C^8–Pt^{1A}–C^7 angle bisector to be considered as a Pt–π bond and the midpoint of the C^8–C^7 double bond as a point ligand, which is common for many square-planar π-complexes of platinum. In the crystallographic packing, the molecules of the complex form chains parallel to the axis a

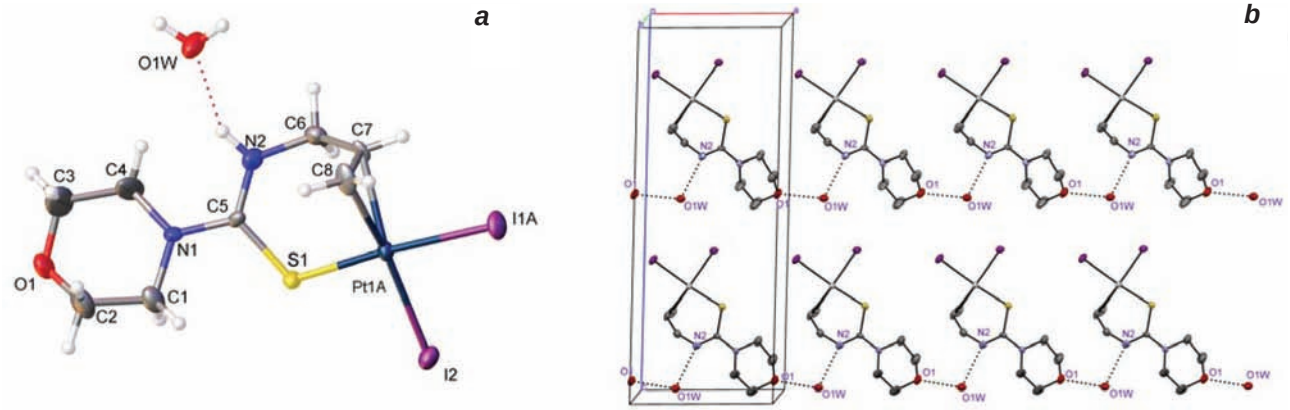

*Fig. 2. Molecular structure (**a**) and packing diagram (**b**) of the complex **I**; thermal ellipsoids are shown at 50% probability level; hydrogen atoms are omitted (in packing diagram) for clarity*

(Fig. 2, *b*) due to hydrogen bonds $O^{1W}H\ldots O^{1}$ (1.91 Å) and $N^{2}H\ldots O^{1W}$ (1.98 Å). Unfortunately, the crystals of complex **II** were not suitable for X-ray structural studies. However, in our previous publications by correlating the data of X-ray diffraction studies with IR and $^{1}H/^{13}C$ NMR spectra, we showed that these methods are the most favorable for establishing the formation of a π-coordination bond in the synthesized complexes. Therefore, the IR and $^{1}H/^{13}C$ NMR spectral characteristics presented below indicate a similar structure of complex **II**.

UV-Vis spectroscopy. Due to the identical structure of both complexes, their UV-Vis spectra are also similar (Fig. 3, *a*, *b*). They consist of a pronounced absorption band at 327 nm responsible for overlapping of intraligand n→π* and ligand-to-metal charge-transfer (LMCT) transitions (between π-orbitals on I to d-orbitals of platinum, π(I)→d(Pt) [38, 39] as well as metal-to-ligand charge-transfer transitions (between d-orbitals of platinum to π-orbitals on S, d(Pt)→π(S)) and *dd*-electronic transitions with corresponding absorption in the range 370-400 (shoulder-shaped absorption bands) and 442-480 nm.

These absorption bands undergo both bathochromic and hypsochromic shifts of +20/21 and –(10-22) nm relative to their chloride counterparts (green curves in Fig. 2) studied in our previous publications [17, 19]. Such shifts are associated with the influence of the nature of the halogen in the coordination sphere of the metal.

To analyze of complex formation in water-ethanol solution, the dependence of the optical density on the ligand concentration was studied (Fig. 4, *a*, *b*).

The position of the maxima of the absorption bands is slightly different from the previous ones, which is due to the influence of the solvent. They also differ from the position of similar UV-Vis curves when studying complex formation in previous works, which is related to the influence of iodide anions in the system.

The results showed that the titration curves have inflections at the ratio M:L = 1:1, 1:2 and 1:1, 1:3, which indicates the possible coordination of ligands in the solution in both a chelate and non-chelate manner only through the sulfur atoms of the carbothioamide group. The absence of an inflection with a 1:2 ratio of components in the titration curve for complexformation in the system Pt^{2+}-HL^{2} (Fig. 4, *b)* may be due to the effect of the bulky diethyl substituent in HL^{2}. Thus, although the position of the absorption bands is slightly different from chloride complexes, their changes are similar. Despite obtaining complexes in the solid state only with a ratio of 1:1 (which is caused by the Pearson's effect of "molecular antisymbiosis in the trans effect" [40], which we have already indicated in previous works), in solution they can also exist in a ratio of 1:1, 1:2, and 1:3.

IR spectroscopy. In the high-frequency region of the IR spectra of HL^{1} and HL^{2} the absorption bands referring to stretching vibrations of ν(NH), $\nu_{as}(CH_2)_{morph}/\nu_{as}(CH_2, CH_3)_{diethyl}$, $\nu_{s}(CH_2)_{morph}/\nu_{s}(CH_2, CH_3)_{diethyl}$ and $\nu(CH)_{allyl}$ are present [41-43]. In the IR spectra of complexes **I**, **II** the ν(NH) and $\nu_{as/s}(CH)$ allyl bands are significantly shifted (Δν = +51/25 and +49/44 cm^{-1}) to higher frequencies which is caused by the involvement of carbothioamide and allyl moieties in the formation of a coordination bond with a metal ion (see Fig. 5 and Experimental section, where the assignments of the characteristic absorption bands).

At the same time, the absorption bands $\nu_{as}(CH_2)_{morph}/\nu_{as}(CH_2, CH_3)_{diethyl}$ of the morpholine ring and the diethylamine fragment shift slightly only by Δν = 5-10 cm^{-1}. However, the vibrations ν(CS) undergo a low-frequency shift by 15/45 cm^{-1}, which is characteristic of the chelate coordination of the carbothioamide group with participation (C=S) in the formation of the metal cycle.

NMR Studies. The comparison of the ^{1}H NMR spectra of the starting thioureas $HL^{1,2}$ with n,π-chelate complexes **I**, **II** (Fig. 5, Table 1) shows a significant downfield shift of the proton signals of NH groups ($\Delta\delta_H$ = +1.37/1.34 ppm) and the upfield shift of the proton signals of allylic fragment ($=C^{8}H_{trans}$, $=C^{8}H_{cis}$, $-C^{7}H=$ by $\Delta\delta_H$ = -(0.5–0.85/-0.42–0.68) ppm), which are part of the six-membered metallocycle with formation of a π-coordination bond ($(C^{8}=C^{7})\rightarrow Pt$ (Scheme 1). These signal shifts are analogous to the chloride counterparts of these complexes synthesized by us earlier [16, 18, 19]. However, unlike chloride complexes, the values of these shifts are smaller, which is due to the lower electronegativity of iodide anions compared to chloride ones. This indicates that both the formation of the π-coordination bond and the nature of the halogen in the coordination environment of the metal significantly affect the position of the signals in the NMR spectra.

Another characteristic spectral feature that indicates the formation of a metallocycle is the splitting of a wide and poorly split multiplet (at 4.17 ppm

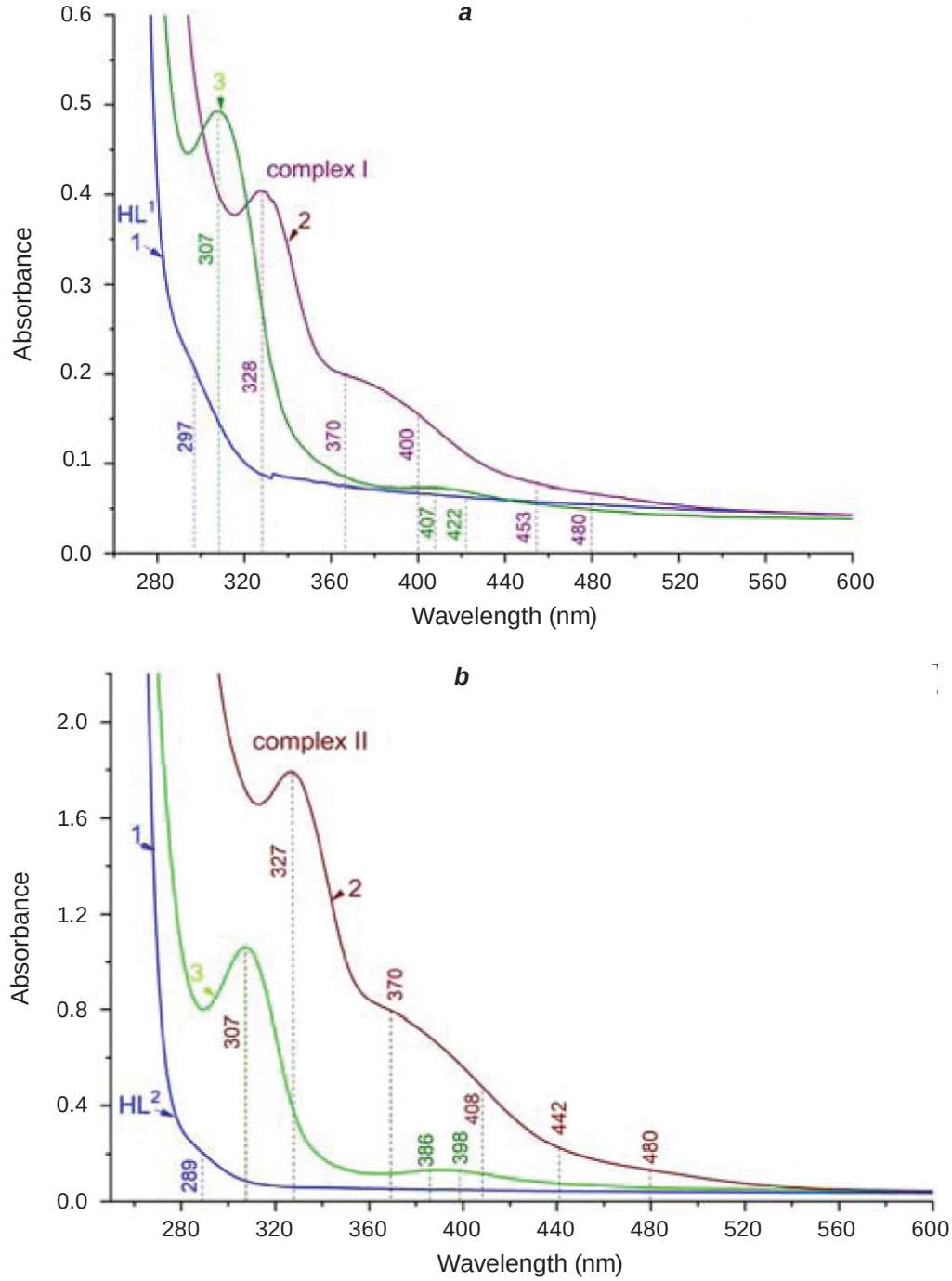

*Fig. 3 The UV–vis spectra of complexes **I (a), II (b)** in DMF-ethanol (1:5) solution and their comparison with the spectra of chloride analogues: 1 – the UV–vis spectra of thioureas HL^1, HL^2 in DMF-ethanol (1:5); 2 – complexes **I**, **II**; 3 – analogs chloride complexes*

in ^{1}H NMR free ligand) into two doublets with appropriate constants of spin-spin interaction due to the axial and equatorial arrangement of protons at carbon C^6 (Fig. 6). In the ^{13}C NMR spectra of the complexes, the signals of carbons C^8, C^7, and C^5 undergo the most significant shift in relation to the starting thioureas (Fig. 7). At the same time, the participation of C^5=S in coordination to the central metal ion determines the upfield chemical shift of C^5 only by $\Delta\delta_C$ = -(12.13–15.15) ppm. Instead, the participation of C^8=C^7 in the formation of a π-acceptor bond with a metal ion causes a significant chemical

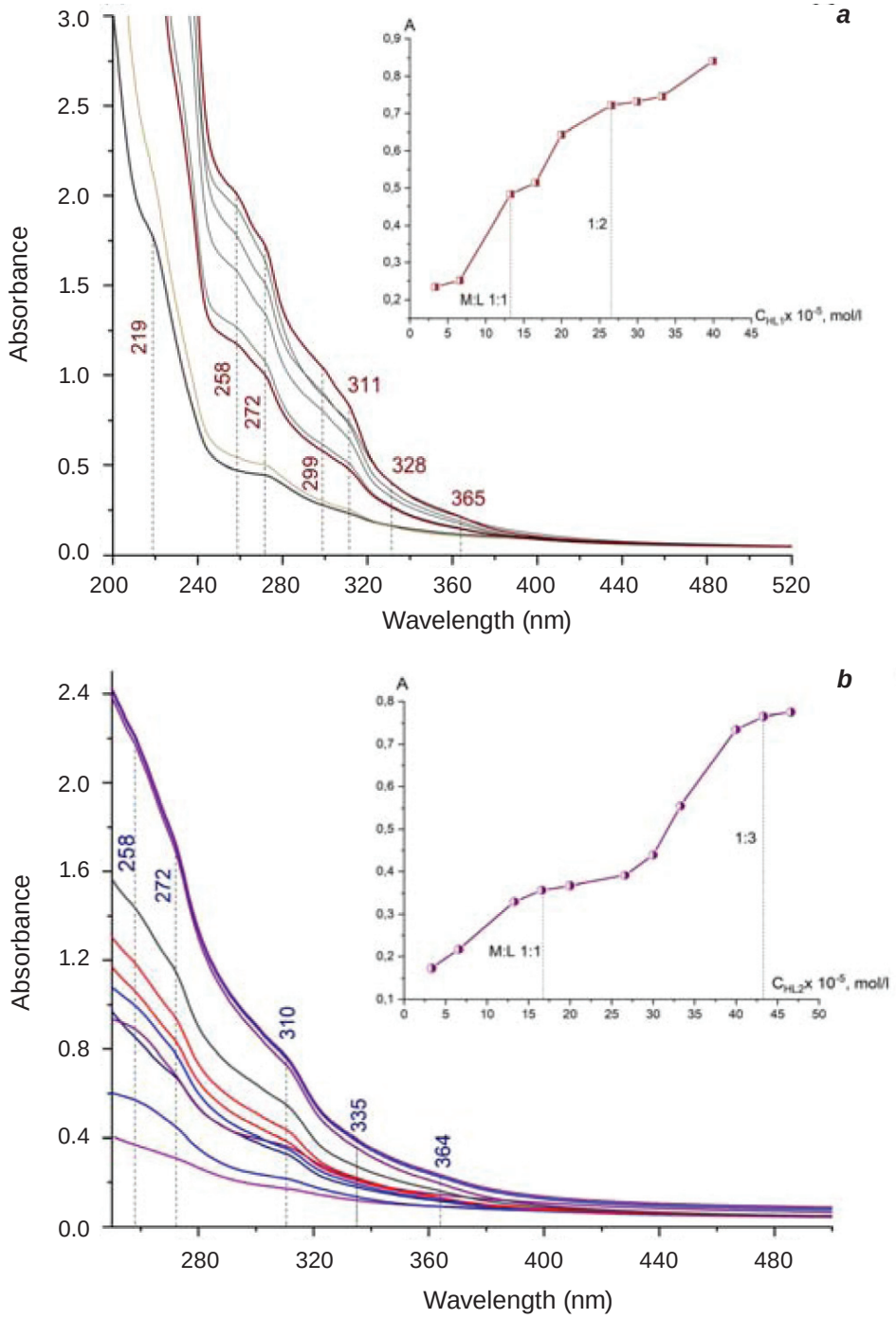

*Fig. 4 The UV-Vis spectra and titration curves for complex formation in the systems Pt^{2+}-HL^1 (**a**) and Pt^{2+}-HL^2 (**b**) in the water-ethanol solutions*

shift of the signals of these carbons (($\Delta\delta_C$ = -(50.82–55.10) ppm) in the upfield, which is also indicative for establishing the structure similar compounds [16, 18].

Similar to the previous spectra, the values of chemical shifts of carbons are slightly smaller compared to ^{13}C NMR spectra of chloride analogs. The given spectral changes indicate that the obtained π-complexes are stable in DMSO, and the ^{1}H/^{13}C NMR method is convenient for the study of such kinds of compounds.

Study of the influence of complexes I, II on the activity of hepatobiliary system enzymes in comparison with their chloride analogs. In order to obtain

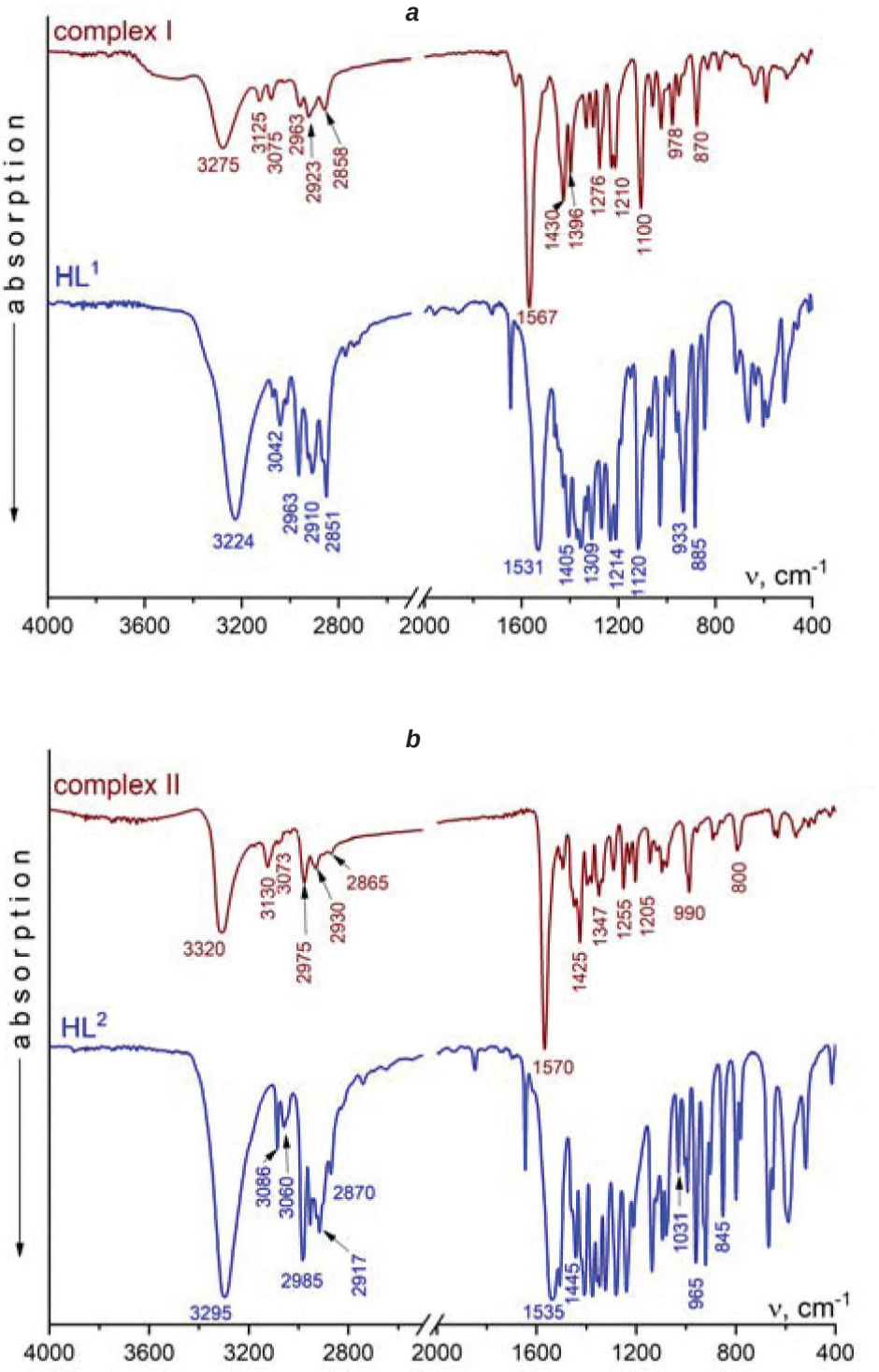

Fig. 5. IR spectra of starting HL[1], HL[2] and complexes ***I, II***

the most extensive information about the effect of synthesized n,π-chelate complexes of Pt(II) based on N-allylthioureas on the metabolic indicators of HepG2 cells, the activity of a number of enzymes (such as alanine aminotransferase (ALT), aspartate aminotransferase (AST), lactate dehydrogenase (LDH), gamma-glutamyl transpeptidase (GGT)) and the level of glucose absorption were investigated. These indicators reflect the response of these cells to treatment. In this subsection, for the first time, we

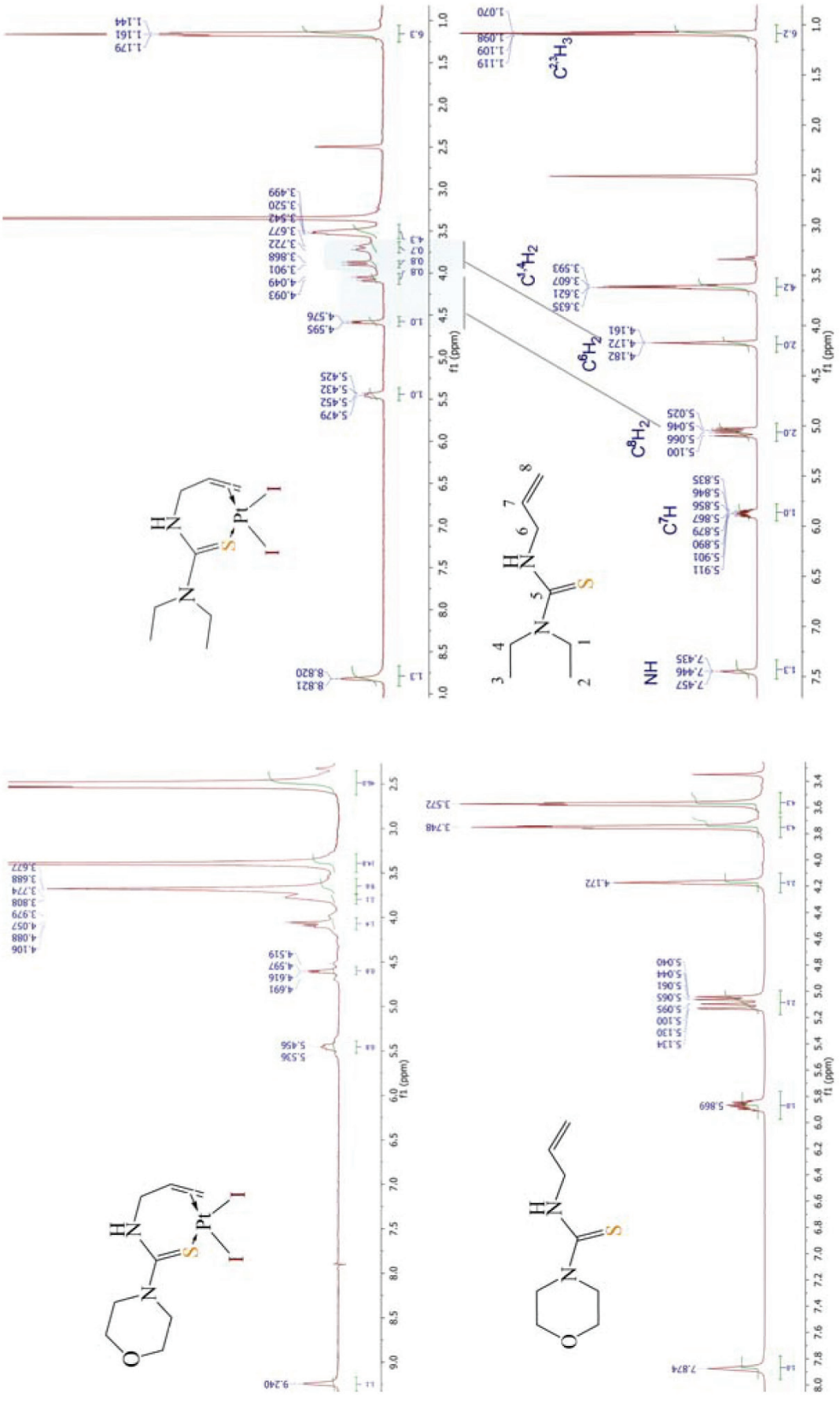

*Fig. 6 ^{1}H NMR spectra of starting HL^1, HL^2 and complexes **I**, **II** in DMSO-d_6*

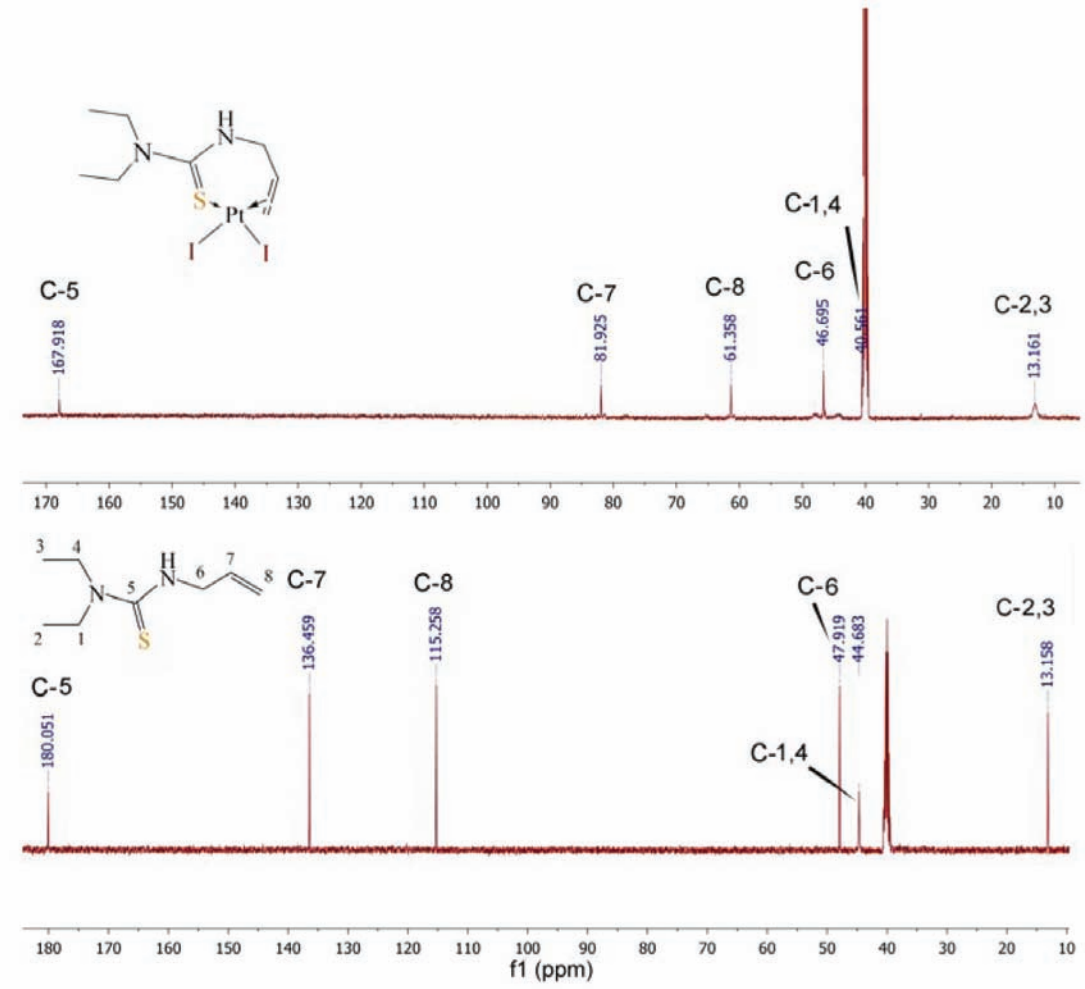

*Fig. 7. ^{13}C NMR spectra of starting HL^2 and complex **I***

present studies not only for complexes **I**, **II**, but also for their previously synthesized analogs $[Pt(HL^1)Cl_2]$ (**III**) and $[Pt(HL^2)Cl_2]$ (**IV**) [16]. Although the chloride analogs of these complexes were synthesized earlier, their effect on the enzymes of the hepatobiliary system was investigated in this work for the first time. Therefore, in the presented experiments, the effect of new iodide π-complexes is compared with the effect of their chloride analogs and with cisplatin.

Determination of the IC_{50} for complexes **I** and **II** was carried out using the MTT test on Hela cells, according to the same algorithm as for complexes **III** and **IV** [16]. The cytotoxic/cytostatic effect of complexes **I** and **II** was also studied using Hela cells. The complexes were titrated in the concentration range of 0.00078-1.6 mmol. As can be seen from Fig. 8, the IC_{50} indicators for the studied complexes were 3×10^{-5} M (**I**) and 5×10^{-6} M (**II**), while for chloride analogs, these indicators were 1×10^{-5} M (**III**) and 2.5×10^{-5} M (**IV**) respectively. Thus, complex **II** showed the highest cytotoxic activity. According to the cytotoxic effect, the compounds can be placed in the following sequence: **II** > **III** > **IV** > **I** > cisplatin.

In further studies of metabolic indicators, HepG2 cells were used under the influence of substances at a concentration of $IC_{50}/10$. (The decrease in the concentration of the test substances relative to the determined IC_{50} index is carried out in order to evaluate the initial effects of the active substance, since if we are talking about the cytotoxic effect, then it is 50% of dead cells compared to the control, and accordingly, the mechanism of influence, especially with regard to metabolic, enzymatic effects, cannot be estimated. Therefore, it is expedient to reduce the concentration relative to the IC_{50} indicator). The results of determining the activity of ALT and AST showed that both iodide n,π-chelate complexes **I** and **II** significantly reduce the level of these en-

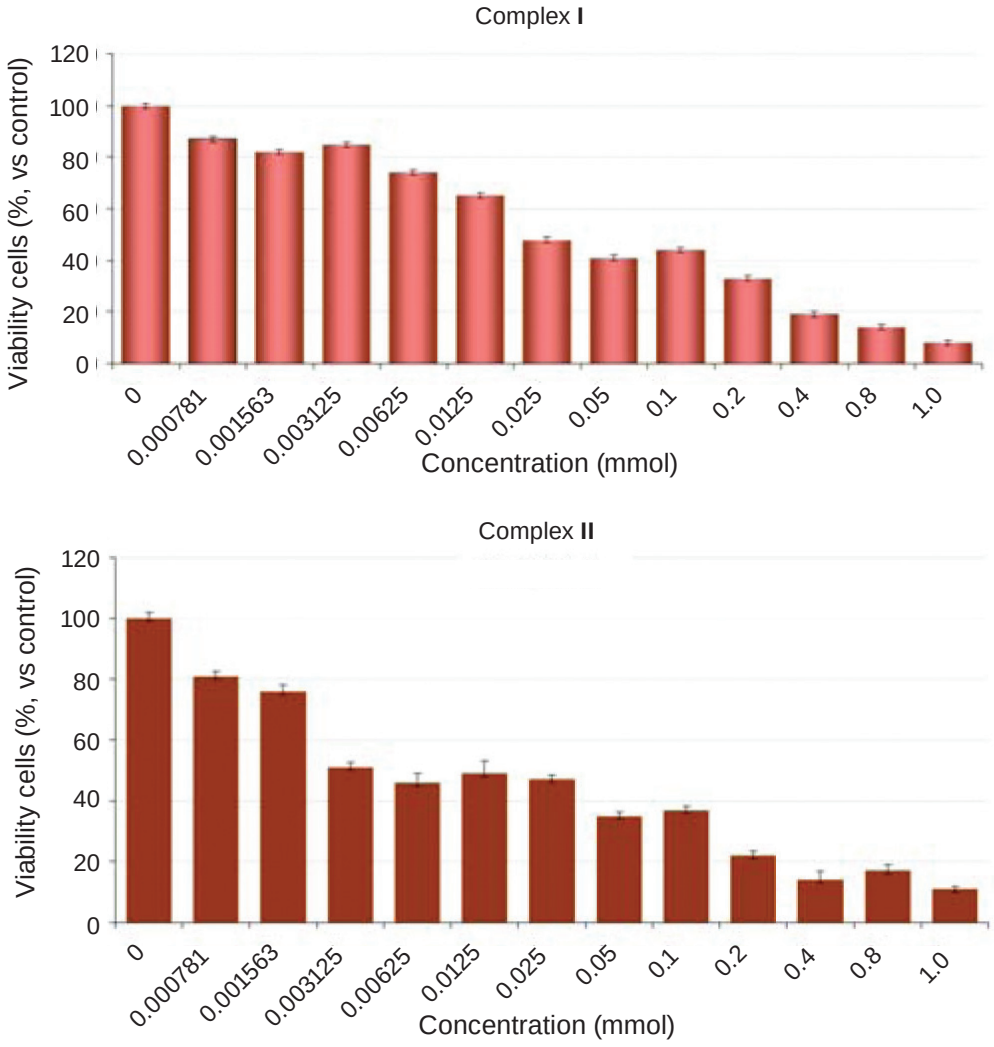

*Fig. 8. Determination of IC_{50} for complexes **I** and **II** in the concentration range of 0.00078–1.6 mmol in the cytotoxic/cytostatic MTT test using Hela cells*

zymes, while chloride analogs had an alternative effect on the enzymes: complex IV increased ALT activity, both in comparison with cisplatin and control, while complex **III** inhibited ALT activity compared to the control (Fig. 9, *a*).

The opposite effect of chloride n,π-chelate complexes is observed on AST: complex **III** increased the activity of this enzyme relative to control and cisplatin, while complex IV inhibited it relative to control and almost did not differ in its effect from cisplatin (Fig. 9, *b*).

Thus, complex **IV** was the most effective when acting on ALT level, while complex **III** – when acting on AST activity. Based on this, we can say that despite the identical structure of the investigated compounds, their activity strongly depends on the composition. The presence of iodide anions in the coordination environment of metals neutralizes the effect of organic ligands and inhibits the activity of both enzymes, while the activity of chloride complexes depends on the nature of the organic ligand.

An acidic environment is observed in tumor cells, which is caused by the high activity of the LDH enzyme. This phenomenon is observed when the enzyme initiates the synthesis of lactate from pyruvate. Lowered pH promotes the activation of anaerobic respiration (glycolysis in conditions of hypoxia) and at the same time blocks the activation of cell apoptosis. When LDH is switched to pyruvate synthesis, the pH does not decrease and thus increases the level of apoptotic cells. Cisplatin reduces the level of LDH, in the test (Fig. 10, *a*). Most

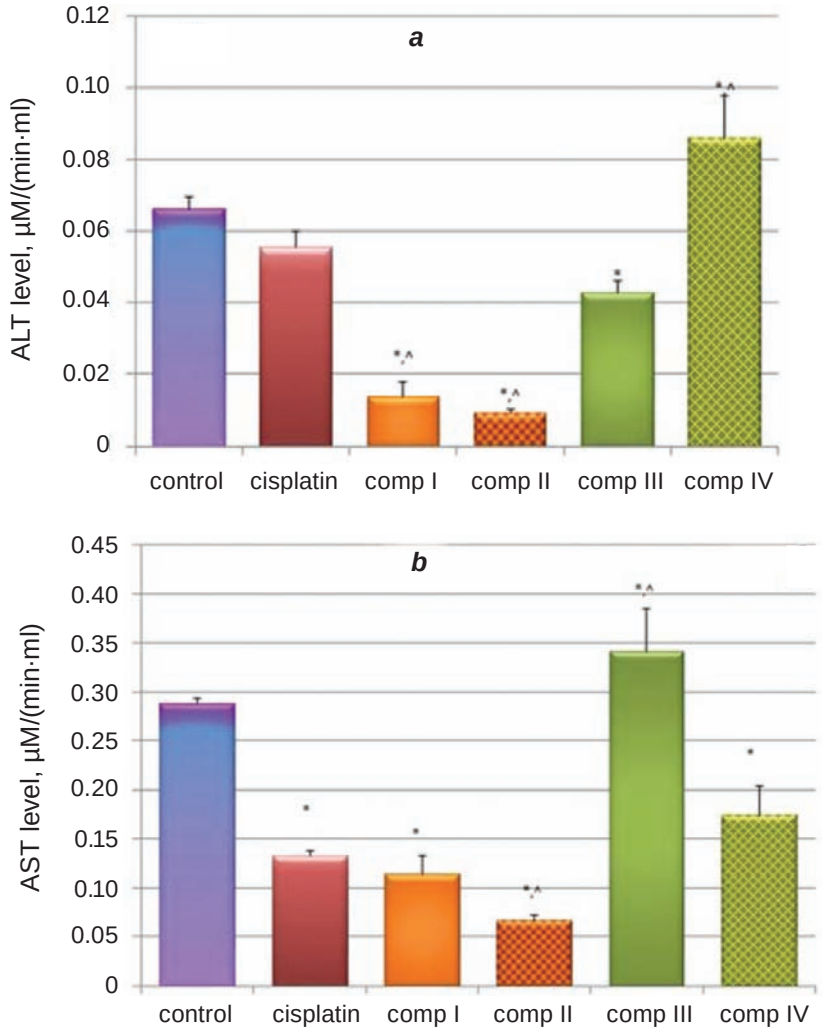

*Fig. 9. Activity of ALT(**a**) and AST (**b**) in the microenvironment of HepG2 cells under the influence of cisplatin and Pt(II) π-complexes **I-IV**. *P < 0.05 – compared to control; ^P < 0.05 – compared to cisplatin*

likely, this means that conditions for glycolysis deteriorate in the cell and create conditions for tissue respiration, which occurs at normal pH. In comparison with the corresponding control and cisplatin, under the influence of complex I, both LDH activity and glucose absorption by cells decrease (Fig. 10, *a*, *b*). On the contrary, complex **II** increases the activity of both LDH and the absorption of glucose by cells. Like complex **I**, chloride compounds **III** and **IV** also inhibit lactate synthesis. However, complex **I** turned out to be the most effective, under the influence of which the level of LDH activity is reduced by almost half, thereby providing better conditions for the transition of cells to tissue respiration. Thus, according to the effectiveness of the influence on the activity of LDH and the level of glucose absorption, the studied compounds should be placed in the following sequence: **I** > **III** > **IV** > **II**. In these studies, the most effective iodide and chloride n,π-chelate complexes based on N-allylmorpholine-4-carbothioamide (HL^1).

In HepG2 cells of hepatocyte line, glucose absorption increases under the influence of complex **II** (Fig. 10, *b*). This effect can be caused by the presence of a bulky diethyl substituent and iodide anions in the complex, which are characterized by a much larger radius compared to chloride anions. As a result, when such a complex enters the cell, it leaves pores in the cell membrane, thereby increasing glucose uptake by the cell by facilitated diffusion. Such an effect is also observed for the chloride analog **IV**, although the absorption level does not exceed the control limits (Fig. 10, *b*). In contrast to the bulky diethyl substituent of HL2 (in complexes **II** and **IV**),

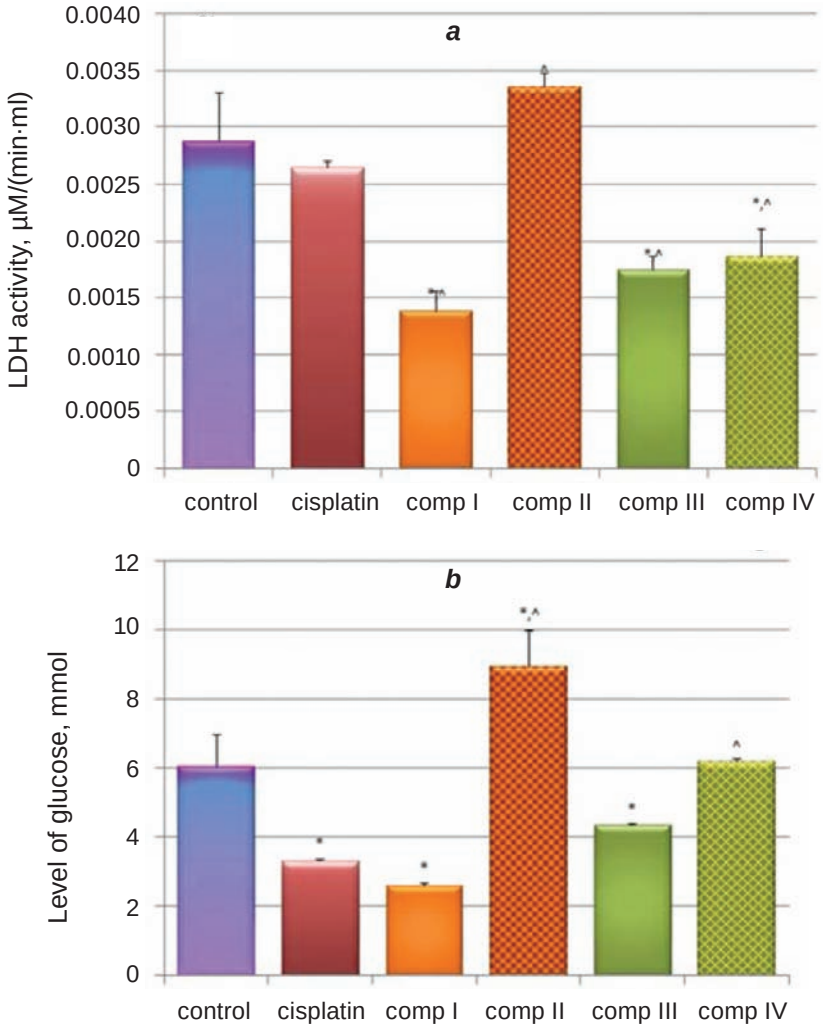

Fig. 10. LDH activity in the microenvironment of HepG2 cells under the influence of cisplatin and Pt(II) π-complexes ***I-IV*** *(**a**). The effect of Pt(II) complexes and cisplatin on the level of glucose utilization by HepG2 cells (**b**). *P < 0.05 – compared to control; ^P < 0.05 – compared to cisplatin*

the morpholine ring of HL1 (in complexes **I** and **III**) has an equatorial-chair conformation (according to X-ray structural data), due to which binding to membrane structures probably does not create such pores that could facilitate the entry of glucose into the cell. The activation of tissue respiration with the participation of glucose is also evidenced by a 2-fold decrease in the level of glucose absorption (under the influence of complex **I**) and 1.5-fold (under the influence of complex **III**) relative to the control. Compounds **I** and **III** probably inhibit anaerobic glycolysis and switch the cell to tissue respiration, reducing glucose absorption. If the activity of succinate dehydrogenase, as the main marker enzyme of mitochondria, is increased, and the activity of LDH is simultaneously switched to the synthesis of pyruvate, we can state the activation of tissue respiration and the possibility of activation of apoptosis [44]. Glucose transport occurs along a concentration gradient and is mediated by transporter proteins.

Determination of the activity of mitochondrial enzymes by the MTT test relative to the number of living cells per 1000 showed a decrease in activity due to the action of cisplatin and complex **II**, and an increase in the activity of mitochondrial enzymes in HepG2 cells under the influence of complexes **I, III** and **IV** (Fig. 11, *a*). Thus, mitochondrial respiration is activated under the action of π-complexes **I**, **III** and **IV**, which is indicated by an increase in the activity of reduced formazan in relation to cell units (Fig. 11, *a*). Compounds **I** and **III** most effectively increase the MTT activity, which indicates

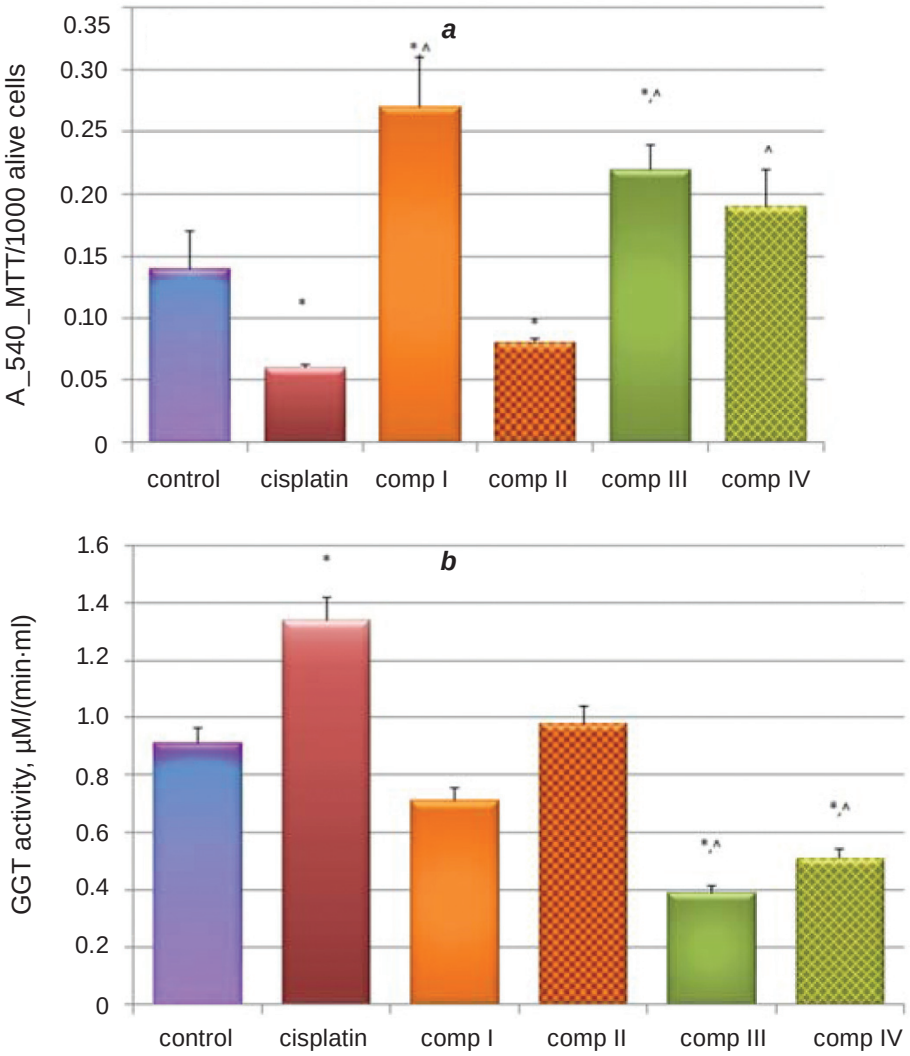

*Fig. 11. The level of reduced 3-(4,5-dimethylthiazol-2-yl)-2,5-diphenyltetrazolium bromide (MTT) to crystalline formazan per unit of living cells (**a**) and GGT activity in the microenvironment of HepG2 cells under the action of cisplatin and π-complexes Pt(II) (**b**). *P < 0.05 – compared to control; ^P < 0.05 – compared to cisplatin)*

the activation of the mitochondrial marker enzyme succinate dehydrogenase. 3-(4,5-dimethylthiazol-2-yl)-2,5-diphenyltetrazolium bromide (MTT) is the main substrate for 90% of succinate dehydrogenase, which is the main enzyme of the inner membrane of mitochondria.

The existing paradigm regarding resistance of tumor cells to anticancer drug treatment is due to a variety of factors, including individual variation in patients and genetic differences of somatic cells in tumors, even those of identical origin [45, 46]. The most common reason for the acquisition of resistance to a wide range of anticancer drugs is the expression of one or more energy-dependent transporters that remove anticancer drugs or their metabolites from cells, which involves other mechanisms of resistance, including insensitivity to apoptosis [47].

When determining the activity of investigated compounds on HepG2 hepatocyte cells, inhibition of GGT activity under the influence of π-complexes **I**, **III** and **IV** was recorded, which can be considered as the ability of these complexes not to cause drug resistance characteristic of cisplatin (Fig. 11, *b*). At the same time, complexes **III** and **IV** have 2.3- and 1.7-fold inhibition of GGT activity compared to the control. Thus, according to the level of influence on GGT activity, complexes can be placed in the following sequence: **III** > **IV** > **I**. Cisplatin

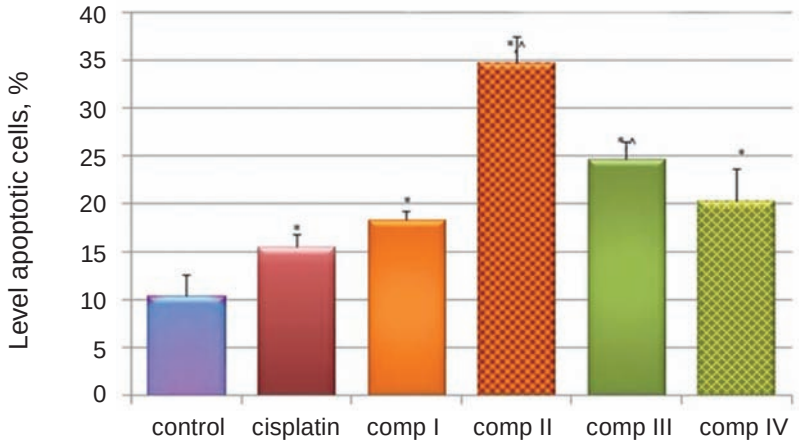

*Fig. 12. The level of apoptotic cells under the influence of cisplatin and complexes **I-IV**.*P < 0.05 – compared to control; ^P < 0.05 – compared to cisplatin*

and complex **II** did not inhibit GGT activity. Thus, complexes **I**, **III** and **IV** are most able to prevent the formation of drug resistance, which is characteristic of the classic anticancer drug cisplatin.

The most effective mechanism for stopping the growth of cancer cells is the activation of the apoptosis system. The effectiveness is due to the unique intercalating properties of cisplatin, which enters the cell and forms several different "DNA-platinum" adducts, thereby initiating the cellular self-defense system by activating or silencing various genes, leading to apoptosis. Our preliminary results of agarose gel electrophoresis studies also showed the DNA binding ability of the studied π-coordination compounds [16]. In addition, previous molecular docking showed that, unlike cisplatin, the presence of an electron-donor atom not involved in coordination contributed to the interaction of the complexes not only with the guanidine fragment of DNA (with the GG pocket), but additionally with the adenine fragment (with the GA pocket) [18]. Consequently, under the influence of the investigated compounds the level of apoptotic cells, compared to the control, increases by 1.8 (for **I**), 3.5 (for **II**), 2.5 (for **III**) and 2.0 times (for complex **IV**) (Fig. 12).

The obtained results indicate that the studied compounds are better cytostatics than cisplatin. This may be due to the presence in the composition of complexes of donor centers not involved in coordination (the oxygen atom in the morpholine ring of HL^1) or branched alkyl substituent (diethylamine fragment in HL^2), which can form additional hydrogen bonds with DNA molecule causing greater stability of such compounds. In addition, we have shown that the activity of n,π-chelate complexes is determined not only by the nature of the substituent in the organic ligand, but also by the nature of the halide anions in the coordination environment of the metal. For the most part, the effect of the studied complexes **I**, **III** and **IV** is reduced to a decrease in the degree of malignancy of cells of hepatocyte lines and the activity of LDH and GHT, as well as a decrease in consumed glucose.

Conclusion. Two new n,π-chelate complexes of platinum(II) with iodide anions in the coordination sphere title $[Pt(HL^{1,2})I_2]\times nH_2O$ (n = 1, 0; $HL^{1,2}$ – N-allylmorpholine-4-carbothioamide or 3-allyl-1,1-diethylthiourea) are presented for the first time. Their IR, UV-Vis and $^1H/^{13}C$ NMR spectral characteristics, as well as influence on the activity of enzymes of the hepatobiliary system and the process of glycolysis were studied in compared with cisplatin and their chloride analogs $[Pt(HL^{1,2})Cl_2]$ synthesized earlier.

The structure of complex **I** (based on HL^1) was described by single-crystal X-ray diffraction study. It was established that both iodide complexes have a structure similar to their chloride counterparts: ligand molecules $HL^{1,2}$ in all the complexes are coordinated in a bidentate manner via the sulfur atom of the thiourea group and the C=C double bond of the allyl moiety with the formation of the π-coordination bond and stable six-membered chelate metallocycle; iodide anions occupy the cis-position in the square-planar coordination sphere of the metal. The main indicator of π-coordination bond forming in $^1H/^{13}C$ NMR spectra is significant shift of the C^7 and C^8

carbon signals in the ^{13}C NMR as well as splitting of the proton multiplet of the C^6H_2-group of the allyl moiety into two doublets (in the ^1H NMR spectra).

The study of the UV-Vis spectra of dissolved complexes in the mixture of ethanol and DMF showed that the absorption bands undergo both bathochromic and hypsochromic shifts relative to their chloride counterparts caused by the influence of the nature of the halogen in the coordination sphere of the metal. Studies of complex formation in water-ethanol solution have shown that the metal–ligand interaction occurs at a M:HL ratio of 1:1, 1:2 and 1:3, which is possible only in the case of monodentate coordination of the ligand HL; this does not occur for the complexes in the solid state due to Pearson's effect of "molecular antisymbiosis in the trans effect".

Biological studies showed that the platinum iodide n,π-chelate complex **II** based on the 3-allyl-1,1-diethylthiourea showed the highest cytotoxic/cytostatic effect compared to all chloride analogs. In general, all complexes showed a greater cytotoxic/cytostatic effect in comparison with their clinical analog cisplatin. According to IC_{50} indicators, all the studied compounds should be placed in the following sequence: $[Pt(HL^2)I_2]$ (**II**) > $[Pt(HL^2)Cl_2]$ (**IV**) > $[Pt(HL^1)Cl_2]$ (**III**) > $[Pt(HL^1)I_2]$ (**I**) > cisplatin.

However, when determining the main indicators of the hepatobiliary system (when studying the influence of complexes on the ALT and AST activity), it was established that the most effective were chloride complexes **III** and **IV**: compounds **III** and **IV** significantly increased the activity of AST and ALT, respectively, while iodide complexes inhibited the activity of these enzymes. Instead, LDH activity and, accordingly, glucose uptake by HepG2 cells was the highest under the influence of complex **I**, however, the reduction of MTT to Formazan crystals by living cells was significantly lower than in the control and under the influence of cisplatin. For complexes **I**, **III** and **IV**, a decrease in LDH activity and glucose absorption was recorded compared to the control, as well as a decrease in LDH activity compared to cisplatin. According to the effectiveness of the influence on the activity of LDH and the level of glucose absorption, the studied compounds should be placed in the following sequence: **I** > **III** > **IV** > **II**. In these studies, the most effective iodide and chloride n,π-chelate complexes based on N-allylmorpholine-4-carbothioamide (HL^1).

Studies of the effect of target complexes on GGT activity, as a key marker of the formation of drug resistance, showed that the compounds inhibit the activity of this enzyme in the following sequence: **III** > **IV** > **I**. Cisplatin and complex **II** did not inhibit GGT activity. Thus, complexes **I**, **III** and **IV** are most able to prevent the formation of drug resistance, which is characteristic of the classic anticancer drug cisplatin. For all studied complexes, a proapoptotic effect on HepG2 cells was recorded in comparison with the control. The obtained data indicate that the compounds **I**, **III** and **IV** are the most promising for further preclinical testing.

Conflct of interest. Authors have completed the Unified Conflicts of Interest form at http://ukrbiochemjournal.org/wp-content/uploads/2018/12/coi_disclosure.pdf and declare no conflict of interest.

Funding. This research was supported by the National Academy of Sciences of Ukraine (according to fundamental research on the topic 321 E of the V.I. Vernadsky Institute of General and Inorganic Chemistry of the National Academy of Sciences of Ukraine).

Acknowledgment. The authors are grateful to the Limited Liability Company Research and Production Enterprise ENAMINE (ENAMINE LTD for providing the opportunity to record ^{13}C NMR spectra.

ЙОДИДНІ n,π-ХЕЛАТНІ КОМПЛЕКСИ ПЛАТИНИ(II) НА ОСНОВІ N-АЛІЛЗАМІЩЕНИХ ТІОСЕЧОВИН ТА ЇХ ВПЛИВ НА АКТИВНІСТЬ ЕНЗИМІВ ГЕПАТОБІЛІАРНОЇ СИСТЕМИ У ПОРІВНЯННІ З ХЛОРИДНИМИ АНАЛОГАМИ

В. Орисик[1]✉, Л. Гарманчук[2], С. Орисик[3], Ю. Зборовський[1], С. Шишкіна[4], І. Ступак[2], П. Новікова[3], Д. Остапченко[2], Н. Храновська[5], В. Пехньо[3], М. Вовк[1]

[1]Інститут органічної хімії НАН України, відділ хімії функціональних гетероциклічних систем, Київ;
[2]ННЦ «Інститут біології та медицини», Київський національний університет імені Тараса Шевченка, кафедра біомедицини, Україна;
[3]Інститут загальної та неорганічної хімії ім. В.І. Вернадського НАН України, відділ хімії комплексних сполук, Київ;
[4]Науково-технологічний комплекс «Інститут монокристалів» НАН України, відділ рентгеноструктурних досліджень та квантової хімії ім. О. В. Шишкіна, Харків;
[5]Національний інститут раку, Київ, Україна;
✉e-mail: vis.viktorys@gmail.com

Пошук нових ефективних препаратів у лікуванні новоутворень залишається актуальним і сьогодні, оскільки адаптація трансформованих клітин до дії класичних препаратів сприяє виникненню лікарської резистентності. Це стосується ряду класичних хіміопрепаратів платинового ряду, зокрема цисплатину. У даній роботі ми описуємо дію нових аналогів цисплатину на клітини HepG2 і на ключовий ензим системи антиоксидантного захисту гамма-глутамілтранспептидазу (ГГТ), яка відіграє важливу роль у набутті патогенними клітинами лікарської стійкості до протипухлинних препаратів. Як аналоги цисплатину отримано нові моноядерні йодидні n,π-хелатні комплекси Pt(II) із заміщеними тіосечовинами N-алілморфолін-4-карботіоамідом або 3-аліл-1,1-діетилтіосечовиною. Усі сполуки досліджено спектральними методами ЕСП, ІЧ та $^{1}H/^{13}C$ ЯМР. Комплекс **I** описано за допомогою рентгеноструктурного дослідження монокристалів. Також досліджено вплив цих аналогів на аланінамінотрансферазу (АЛТ), аспартатамінотрансферазу (ААТ), лактатдегідрогеназу (ЛДГ), які є маркерними ензимами при діагностиці захворювань печінки. Всі дослідження проведені у порівнянні зі хлоридними n,π-хелатними комплексами платини, отриманими раніше (однак вплив цих хлоридних аналогів платини на зазначені ензими досліджено вперше). Встановлено, що за показником IC_{50} і рівнем апоптозу клітин HepG2 досліджувані сполуки перевищують цисплатин. Крім того, дія досліджуваних комплексів здебільшого зводиться до зниження ступеня малігнізації клітин ліній гепатоцитів та активності ЛДГ і ГГТ, а також до зниження спожитої глюкози.

Ключові слова: n,π-хелати; тіосечовини, спектроскопія ЯМР; кристалічна структура, гамма-глутамілтранспептидаза, аланін амінотрансфераза, аспартатамінотрансфераза, лактатдегідрогеназа.

References

1. Deo KM, Pages BJ, Ang DL, Gordon CP, Aldrich-Wright JR. Transition Metal Intercalators as Anticancer Agents-Recent Advances. *Int J Mol Sci*. 2016; 17(11): 1818.
2. Frezza M, Hindo S, Chen D, Davenport A, Schmitt S, Tomco D, Dou QP. Novel metals and metal complexes as platforms for cancer therapy. *Curr Pharm Des*. 2010; 16(16): 1813-1825.
3. Ndagi U, Mhlongo N, Soliman ME. Metal complexes in cancer therapy - an update from drug design perspective. *Drug Des Devel Ther*. 2017; 11: 599-616.
4. Trudu F, Amato F, Vaňhara P, Pivetta T, Peña-Méndez EM, Havel J, Appl J. Coordination compounds in cancer: Past, present and perspectives. *J Appl Biomed*. 2015; 13: 79-103.
5. Lazarevic T, Rilak A, Bugarčić ŽD. Platinum, palladium, gold and ruthenium complexes as anticancer agents: Current clinical uses, cytotoxicity studies and future perspectives. *Eur J Med Chem*. 2017; 142: 8-31.
6. Pattan SR, Pawar SB, Vetal SS, Gharate UD, Bhawar SB. The scope of metal complexes in drug design - A review. *Indian Drugs*. 2012; 49(11): 5-12.
7. Martín J, Alés MR, Asuero AG. An overview on ligands of therapeutically interest. *Pharm Pharmacol Int J*. 2018; 6(3): 198-214.
8. Selvaganapathy M, Raman N. Pharmacological Activity of a Few Transition Metal Complexes:

A Short Review. *J Chem Biol Ther*. 2016; 1(2): 108.
9. Tripathi L, Kumar P, Singhai AK. Role of chelates in treatment of cancer. *Indian J Cancer*. 2007; 44(2): 62-71.
10. Zuccolo M, Arrighetti N, Perego P, Colombo D. Recent Progresses in Conjugation with Bioactive Ligands to Improve the Anticancer Activity of Platinum Compounds. *Curr Med Chem*. 2022; 29(15): 2566-2601.
11. Bajracharya R, Song JG, Patil BR, Lee SH, Noh HM, Kim DH, Kim GL, Seo SH, Park JW, Jeong SH, Lee CH, Han HK. Functional ligands for improving anticancer drug therapy: current status and applications to drug delivery systems. *Drug Deliv*. 2022; 29(1): 1959-1970.
12. Kumar V, Chimni SS. Recent developments on thiourea based anticancer chemotherapeutics. *Anticancer Agents Med Chem*. 2015; 15(2): 163-175.
13. Mohapatra RK, Das PK, Pradhan MK, El-Ajaily MM, Das D, Salem HF, Mahanta U, Badhei G, Parhi PK, Maihub AA, Kudrat-E-Zahan Md. Recent Advances in Urea- and Thiourea-Based Metal Complexes: Biological, Sensor, Optical, and Corroson Inhibition Studies. *Comments Inorg Chem*. 2019; 39(3): 127-187.
14. Fakhar I, Yamin BM, Hasbullah SA. A comparative study of the metal binding behavior of alanine based bis-thiourea isomers. *Chem Cent J*. 2017; 11(1): 76.
15. Saeed A, Flörke U, Erben MF. A review on the chemistry, coordination, structure and biological properties of 1-(acyl/aroyl)-3-(substituted) thioureas. *J Sulfur Chem*. 2014; 35(3): 318-355.
16. Repich HH, Orysyk VV, Palchykovska LG, Orysyk SI, Zborovskii YuL, Vasylchenko OV, Storozhuk OV, Biluk AA, Nikulina VV, Garmanchuk LV, Pekhnyo VI, Vovk MV. Synthesis, spectral characterization of novel Pd(II), Pt(II) π-coordination compounds based on N-allylthioureas. Cytotoxic properties and DNA binding ability. *J Inorg Biochem*. 2017; 168: 98-106.
17. Borovyk PV, Orysyk SI, Repich HH, Likhanov AF, Mishchenko AM, Zborovskii YuL, Orysyk VV, Palchikovska LG, Pekhnyo VI, Vovk MV. Spectral characteristics and cytostatic effect of Pd(II) and Pt(II)carbothioamide π-complexes on Allium cepa L meristem cells. *Vopr Khim Khim Tekhnol*. 2020; (3): 34-45.
18. Orysyk SI, Baranets S, Borovyk PV, Palchykovska LG, Zborovskii YuL, Orysyk VV, Likhanov AF, Platonov MO, Kovalskyy DB, Shyryna TV, Danylenko Y, Hurmach VV, Pekhnyo VI, Vovk MV. Mononuclear π-complexes of Pd(II) and Pt(II) with 1-allyl-3-(2-hydroxyethyl)thiourea: Synthesis, structure, molecular docking, DNA binding ability and genotoxic activity. *Polyhedron*. 2021; 210: 115477.
19. Orysyk SI, Zborovskii YuL, Orysyk VV, Garmanchuk LV, Borovyk PV, Shishkina SV, Pavliuk O, Pekhnyo VI, Vovk MV. Synthesis, structural and spectral characteristics of novel n,π-chelate complexes of Pd(II) and Pt(II) with N-allylthioureas and their influence on the growth of spheroids cells MCF-7 and GGT activity. *Polyhedron*. 2023; 231: 116272.
20. Bilyuk AA, Storozhuk OV, Kolotiy OV, Repich HH, Orysyk SI, Garmanchuk LV. Pd(II) and Pt(II) complexes influence on spheroids growth of breast cancer cells. *Biotechnol Acta*. 2017; 10(1): 61-67.
21. Otto AM. Warburg effect(s)-a biographical sketch of Otto Warburg and his impacts on tumor metabolism. *Cancer Metab*. 2016; 4: 5.
22. Zhou N, He C-X. An improved method of isomolar series by dual-wavelength spectrophotometry. *Mikrochim Acta*. 1993; 111: 183-191.
23. Sheldrick GM. A short history of SHELX. *Acta Crystallogr A*. 2008; 64(Pt 1): 112-122.
24. Ihrke G, Neufeld EB, Meads T, Shanks MR, Cassio D, Laurent M, Schroer TA, Pagano RE, Hubbard AL. WIF-B cells: an in vitro model for studies of hepatocyte polarity. *J Cell Biol*. 1993; 123(6 Pt 2): 1761-1775.
25. Kamalian L, Chadwick AE, Bayliss M, French NS, Monshouwer M, Snoeys J, Park KB. The utility of HepG2 cells to identify direct mitochondrial dysfunction in the absence of cell death. *Toxicol In Vitro*. 2015; 29(4): 732-740.
26. Vedenicheva NP, Al-Maali GA, Bisko NA, Kosakivska IV, Ostrovska GV, Khranovska NM, Gorbach OI, Garmanchuk LV, Ostapchenko LI. Effect of Cytokinin-Containing Extracts from Some Medicinal Mushroom Mycelia on HepG2 Cells *In Vitro*. *Int J Med Mushrooms*. 2021; 23(3): 15-28.

27. Mosmann T. Rapid colorimetric assay for cellular growth and survival: application to proliferation and cytotoxicity assays. *J Immunol Methods.* 1983; 65(1-2): 55-63.
28. Alley MC, Scudiero DA, Monks PA, Hursey ML, Czerwinski MJ, Fine DL, Abbott BJ, Mayo JG, Shoemaker RH, Boyd MR. Feasibility of drug screening with panels of human tumor cell lines using a microculture tetrazolium assay. *Cancer Res.* 1988; 48(3): 589-601.
29. Nikolaienko TV, Nikulina VV, Shelest DV, Garmanchuk LV. The mechanism of VEGF-mediated endothelial cells survival and proliferation in conditions of unfed-culture. *Ukr Biochem J.* 2016; 88(4): 12-19.
30. Kjeld M. An automated colorimetric method for the estimation of lactate dehydrogenase activity in serum. *Scand J Clin Lab Invest.* 1972; 29(4): 421-425.
31. Friedman RB, Young DS. Effects of disease on clinical laboratory tests, 3rd Edition, AACC Press, Washington, DC 1997.
32. Reitman S, Frankel S. A colorimetric method for the determination of serum glutamic oxalacetic and glutamic pyruvic transaminases. *Am J Clin Pathol.* 1957; 28(1): 56-63.
33. Bergmeyer HU, Hørder M, Rej R. International Federation of Clinical Chemistry (IFCC) Scientific Committee, Analytical Section: approved recommendation (1985) on IFCC methods for the measurement of catalytic concentration of enzymes. Part 2. IFCC method for aspartate aminotransferase (L-aspartate: 2-oxoglutarate aminotransferase, EC 2.6.1.1). *J Clin Chem Clin Biochem.* 1986; 24(7): 497-510.
34. Schumann G, Bonora R, Ceriotti F, Férard G, Ferrero CA, Franck PFH, Gella FJ, Hoelzel W, Jørgensen PJ. et al. IFCC primary reference procedures for the measurement of catalytic activity concentrations of enzymes at 37 degrees C. International Federation of Clinical Chemistry and Laboratory Medicine. Part 5. Reference procedure for the measurement of catalytic concentration of aspartate aminotransferase. *Clin Chem Lab Med.* 2002; 40(7): 725-733.
35. Nicoletti I, Migliorati G, Pagliacci MC, Grignani F, Riccardi C. A rapid and simple method for measuring thymocyte apoptosis by propidium iodide staining and flow cytometry. *J Immunol Methods.* 1991; 139(2): 271-279.
36. Livingstone SE. The Chemistry of Ruthenium, Rhodium, Palladium, Osmium, Iridium and Platinum, Pergamon text in Inorganic Chemistry, Volume 25, University of New South Wales, 1975.
37. Zhan H, Hu Y, Wang P, Chen J. Molecular structures of gas-phase neutral morpholine and its monohydrated complexes: experimental and theoretical approaches. *RSC Adv.* 2017; 7: 6179-6186.
38. Lever ABP. Inorganic Electronic Spectroscopy. Toronto, Canada, American Elsevier Publishing Co., New York, 1968, p. 420.
39. Petrov AI, Lutoshkin MA. TD-DFT assessment of UV-vis spectra palladium and platinum complexes with thiols and disulfides. *J Mol Model.* 2021; 27(6): 152.
40. Pearson RG. Antisymbiosis and the trans effect. *Inorg Chem.* 1973; 12(3): 712-713.
41. Badertscher M, Bühlmann P, Pretsch E. Structure Determination Of Organic Compounds. Tables of Spectral Data. Springer-Verlag Berlin Heidelberg, 2009. 433 p.
42. Socrates G. Infrared and Raman Characteristic Group Frequencies. Tables and Charts, Third ed., by John Wiley & Sons Ltd, 2001. p. 347.
43. Tucureanu V, Matei A, Avram AM. FTIR Spectroscopy for Carbon Family Study. *Crit Rev Anal Chem.* 2016; 46(6): 502-520.
44. Burns JS, Manda G. Metabolic Pathways of the Warburg Effect in Health and Disease: Perspectives of Choice, Chain or Chance. *Int J Mol Sci.* 2017; 18(12): 2755.
45. Hanigan MH. Gamma-glutamyl transpeptidase: redox regulation and drug resistance. *Adv Cancer Res.* 2014: 122: 103-141.
46. Hanigan MH, Gallagher BC, Townsend DM, Gabarra V. Gamma-glutamyl transpeptidase accelerates tumor growth and increases the resistance of tumors to cisplatin *in vivo. Carcinogenesis.* 1999; 20(4): 553-559.
47. Wang X, Zhang H, Chen X. Drug resistance and combating drug resistance in cancer. *Cancer Drug Resist.* 2019; 2(2): 141-160.